**Validation of the protein kinase *Pf*CLK3 as a multi-stage cross species malarial drug target**

Mahmood M Alam[1]*, Ana Sanchez-Azqueta[2]*, Omar Janha[2*], Erika L. Flannery[3], Amit Mahindra[4], Kopano Mapesa[4], Aditya B. Char[5], Dev Sriranganadane[6], Nicolas Brancucci[7], Yevgeniya Antonova-Koch[3], Kathryn Crouch[7], Nelson Victor Simwela[7], Scott B. Millar[7]

Jude Akinwale[7] Deborah Mitcheson[9], Lev Solyakov[8], Kate Dudek[8], Carolyn Jones[8], Cleofé Zapatero[10], Christian Doerig[11], Davis C. Nwakanma[12], Maria Jesús Vázquez[10], Gonzalo Colmenarejo[13], Maria Jesús Lafuente[10], Maria Luisa Leon[12], Paulo H.C. Godoi[6], John M. Elkins[14], Andrew P. Waters[7], Andrew G. Jamieson[4], León Elena Fernandez Alvaro[10], Lisa C. Ranford-Cartwright[5], Matthias Marti[7], Elizabeth A. Winzeler[3], Francisco Javier Gamo[10], Andrew B. Tobin[2#].

1. Wellcome Centre for Integrative Parasitology and Centre for Translational Pharmacology, Institute of Infection Immunity and Inflammation, University of Glasgow, Glasgow G12 8TA, UK.

2. Centre for Translational Pharmacology, Institute of Molecular Cell and Systems Biology, Davidson Building, University of Glasgow, Glasgow G12 8QQ, UK.

3. Skaggs School of Pharmaceutical Sciences, UC Health Sciences Center for Immunology, Infection and Inflammation, University of California, San Diego, School of Medicine, 9500 Gilman Drive, La Jolla, CA 92093. USA.

4. School of Chemistry, Joseph Black Building. University Avenue, Glasgow, G12 8QQ, UK

5. Institute of Biodiversity, Animal Health and Comparative Medicine, College of Medical, Veterinary and Life Science, University of Glasgow, Graham Kerr Building, Glasgow G12 8QQ.

6. Structural Genomics Consortium, Universidade Estadual de Campinas, Campinas, São Paulo, 13083-886, Brazil

7. Wellcome Centre for Integrative Parasitology, University of Glasgow, Glasgow G12 8QQ,

8. Medical Research Council Toxicology Unit, University of Leicester, University road, Leicester LE1 9HN, UK.

9. Department of Molecular Cell Biology, University of Leicester, University Road, Leicester LE1 9HN, UK.

10. Diseases of the Developing World, GlaxoSmithKline, Severo Ochoa 2, 28760 Tres Cantos, Madrid, Spain.

11. Biomedical Science Cluster, School of Health and Biomedical Sciences, Royal Melbourne Institute of Technology, Melbourne VIC 3000, Australia

12. The MRC Unit the Gambia, Atlantic Boulevard, Fajara, Banjul, The Gambia

13. Biostatistics and Bioinformatics Unit, IMDEA Food Institute, Ctra Cantoblanco 8, 28049 Madrid, Spain

14. Structural Genomics Consortium (SGC), Nuffield Department of Clinical Medicine, University of Oxford, Oxford, OX3 7DQ, United Kingdom

*Contributed equally to this work

#Corresponding author

**Short title:** Validation of PfCLK3 as novel protein kinase target in malaria

**Abstract**

The requirement for next generation anti-malarials to be both curative and transmission blocking necessitate the identification of new druggable molecular pathways. Here we identify a selective inhibitor to the *Plasmodium falciparum* protein kinase *Pf*CLK3 which we use in combination with chemogenetics to validate *Pf*CLK3 as a drug target acting at multiple parasite life stages. Consistent with a role for *Pf*CLK3 in RNA splicing, inhibition results in the down-regulation of >400 essential parasite genes. Inhibiting plasmodium CLK3 mediates rapid killing of asexual blood stage *P. falciparum* and blockade of gametocyte development preventing transmission, as well as showing parasiticidal activity against *P. berghei* and *P. knowlesi*. Hence, our data establishes *Pf*CLK3 as a target with the potential to deliver both symptomatic treatment and transmission blocking in malaria.

**Introduction**

Despite artemisinin-based combinations therapies offering effective frontline treatment for malaria there are still over 200 million cases of malaria worldwide per annum resulting in an estimated 0.5 million deaths. This, combined with the fact that there is now clear evidence for the emergence of resistance to not only artemisinin (*1, 2*) but also to partner drugs including piperaquine and mefloquine (*3, 4*) means that there is an urgent need for novel therapeutic strategies to not only cure malaria but also to prevent transmission. Global phospho-proteomic studies on the most virulent species of human malaria, *P. falciparum* have established protein phosphorylation as a key regulator of a wide range of essential parasite processes (*5-8*). Furthermore, of the 65 eukaryotic protein kinases in the parasite kinome (*9*), over half have been reported to be essential for blood stage survival (*8-12*). These studies, together with the generally accepted potential of targeting protein kinases in the treatment of numerous human diseases (*13, 14*), suggests that inhibition of parasite protein kinases might offer a viable strategy for the treatment of malaria (*6, 15*)

To directly test this hypothesis we focused here on one of the four members of the *P. falciparum* cyclin-dependent like ((CLK) protein kinase family, *Pf*CLK3 (PF3D7_1114700), an essential protein kinase in maintaining the asexual blood stage of both *P. falciparum (8, 12)* and *P. berghei* (*10*). In mammalian cells the CLK protein kinase family and the closely-related SRPK family are crucial mediators of multiple phosphorylation events on splicing factors, including serine-arginine-rich (SR) proteins, which are necessary for the correct assembly and catalytic activity of spliceosomes (reviewed in (*16*)). A key member of the human CLK-family is the splicing factor kinase PRP4 kinase (PRPF4B), which homology-based studies have identified as the closest related human kinase to *Pf*CLK3(*17, 18*). PRPF4B plays an essential role in the regulation of splicing by phosphorylation of accessory proteins

associated with the spliceosome complex (*19*). The finding that *Pf*CLK3 can phosphorylate SR proteins *in vitro* (*20*) supports the notion that *Pf*CLK3, like the other members of the *Pf*CLK family (*17*), plays an essential role in parasite pre-mRNA processing (*18*).

***High throughput screen identifies selective PfCLK3 inhibitors***

We established high-throughput inhibition assays for two essential members of the *Pf*CLK family namely *Pf*CLK1 and *Pf*CLK3 **(fig. S1)**. Both of these protein kinases were purified as active recombinant proteins **(fig. S2A)** and used in a high throughput time-resolved florescence resonance energy transfer (TR-FRET) showing robust reproducibility in 1536 assay format ( Z'>0.7) **(fig. S2B-H)**. This assay was used to screen 24,619 compounds, comprised of 13,533 compounds in the Tres Cantos Anti-Malarial Set (TCAMS) (*21*), 1115 in the Protein Kinase Inhibitor Set (PKIS) (*22*) and 9,970 MRCT index library (*23*), at a single dose (10μM). Hits were defined as those compounds that were positioned >3 standard deviations from the mean of the % inhibition distribution curve **(Fig. 1A,B)** and which also showed >40% inhibition. This identified 2579 compounds (consisting of MRCT=250, PKIS=4, TCAMS=2325) which together with the 259 compounds identified as "the kinase inhibitor set" from within the Medicines for Malaria Venture (MMV) box, a collection of 400 anti-malarial compounds (*24*), were used to generate concentration inhibition curves **(Fig. 1C) (table S1)**. Based on the selectivity criteria of more than a >1.5 log fold difference in the negative logarithm of the half maximal inhibition ($pIC_{50}$), 28% of the hits showed specific inhibition of *Pf*CLK1 and 13% specifically inhibited *Pf*CLK3 whilst 23% of the compounds inhibited both *Pf*CLK3 and *Pf*CLK1 with the remainder (36%) being inactive **(Fig. 1C,D) (table S1).** Exemplar molecules from each of these three classes are shown in **fig. S3**.

Highlighted in Figure 1c is TCMDC-135051 which showed the highest selectivity and efficacy for inhibition of *Pf*CLK3. Furthermore, TCMDC-135051 showed ~100 fold lower activity against the closely related human kinase CLK2 (29% sequence identity with *Pf*CLK3) **(table S1)**. Similarly, TCMDC-135051 showed no evidence of interacting with the human orthologue of *Pf*CLK3, PRPF4B. This was seen in thermostability assays, using differential scanning fluorimetry (DSF), where staurosporine, acting as a positive control, increased the melting temperature of PRPF4B by 2.40±0.14$^{o}$C. In contrast, TCMDC-135051 showed no significant change in PRPF4B thermostability **(fig. S4A).** Furthermore, in a mass spectrometry based PRPF4B activity assay the published inhibitor, Compound A (*25*), showed significant inhibition of PRPF4B whereas TCMDC-135051 at concentrations up to 50μM showed no inhibitory activity **(fig. S4B).** In further counter screens, TCMDC-135051 showed no significant activity against the *P. falciparum* protein kinases, *Pf*PKG and *Pf*CDPK1 **(fig. S5A-C).** Thus, TCMDC-135051 showed selective inhibition of *Pf*CLK3 when compared against the closely related human kinases PRPF4B and CLK2, as well as the closest parasite kinase, *Pf*CLK1, and other parasite kinases (*Pf*PKG, *Pf*CDPK1).

TCMDC-135051 is a member of a series of molecules that were contained in the high throughput screen (HTS) with the same chemical scaffold. This series showed similar inhibitory activity against *Pf*CLK3 **(fig. S6).** Note that the TCMDC-135051 is part of the TCAMs and has previously been shown to have anti-parasiticidal activity ($EC_{50}$=320nM) and the structure has previously been published (*21*). Resynthesis of TCMDC-135051 together with nuclear magnetic resonance (NMR) analysis has however determined the correct structure for TCMDC-135051 to be the one shown in Fig. 1C and fig. S3.

**Parasite strains resistant to TCMDC-135051 show mutations in *Pf*CLK3**

We next sought to confirm that *Pf*CLK3 was the target of TCMDC-135051 parasiticidal activity. Exposing *P. falciparum* Dd2 parasites to increasing concentrations of TCMDC-135051, resulted in emergence of three independent lines that showed decreased sensitivity to TCMDC-135051 but no change in sensitivity to chloroquine or artemisinin **(Fig. 2A, Table 1)**. Whole genome sequencing of the three resistant lines revealed mutations in *Pf*CLK3 (lines TM051A and TM051C) and a mutation in the putative RNA processing protein, PfUSP-39 (PF3D7_1317000)(line TM051B, **Table 1, Fig. 2B)**. The resistant clone TM051A, which contained the mutation P196R in the N-terminal region outside the *Pf*CLK3 kinase domain **(Fig. 2B)**, showed the smallest change in sensitivity to TCMDC-135051 (4.2 fold shift in the $EC_{50}$ compared to parental Dd2 parasites). Examination of the *in vitro* enzymatic properties of the P196R mutant found in TM051A did not detect any significant changes in enzyme kinetics or sensitivity to inhibition by TCMDC-135051 compared to the wild type kinase suggesting that this mutation could potentially stabilise the protein or be otherwise involved in the interaction between *Pf*CLK3 and its substrates or regulatory proteins.

The line, TM051C, containing an H259P mutation in *Pf*CLK3 showed the largest degree of resistance to TCMDC-135051 with a shift in the $EC_{50}$ of >11 fold in the death curve **(Fig. 2C, Table 1)**. Evaluation of the enzymatic properties of the H259P mutant revealed that the mutant kinase possessed ~3 times the activity of the wild type kinase whereas the Km for ATP was similar between mutant and wild type kinases **(Fig. 2D,E)**. The fact that H259 resides outside of the kinase domain suggests that this amino acid is within a regulatory region that controls enzymatic activity.

In contrast to the other two resistant lines, TM051B did not contain a mutation in *Pf*CLK3

but rather contained a mutation (F103I) within the putative zinc-finger ubiquitin binding domain of ubiquitin specific peptidase-39 (*Pf*USP39). Importantly, the human and yeast orthologues of *Pf*USP39 (snRNP assembly-defective protein-1 (Sad1)) are members of the deubiquitinase family that are essential components of the U4/U6-U5 tri-snRNP complex necessary for spliceosome activity (*26-28*). The position of the F103I mutation within the zinc-finger ubiquitin binding domain of USP39 may be of significance since this domain has been implicated in the interaction of USP39/Sad1 with the spliceosome (*27*). Hence, the involvement of USP39 in the same pathway/function as *Pf*CLK3, together with the mutations found in *Pf*CLK3 itself in the other two resistant lines, supports the notion that the parasiticidal activity of TCMDC-135051 is via inhibition of *Pf*CLK3.

**Genetic target validation of *Pf*CLK3**

To further confirm *Pf*CLK3 as the target of TCMDC-135051 parasiticidal activity a variant of *Pf*CLK3 was designed that showed reduced sensitivity to TCMDC-135051. To generate this variant, advantage was taken of the highly selective inhibition of *Pf*CLK3 over *Pf*CLK1 shown by TCMDC-135051. By exchanging amino acids within the sub-domain V of the *Pf*CLK3 kinase domain with equivalent residues in the kinase domain of *Pf*CLK1 **(fig. S1)** a variant of *Pf*CLK3 was generated where glycine 449 in *Pf*CLK3 was substituted with a proline residue (G449P) **(Fig. 3A)**. This recombinant variant protein showed a ~3 fold log shift in sensitivity for inhibition by TCMDC-135051 **(Fig. 3B,C)** (*Pf*CLK3 $pIC_{50}$=7.35±0.12 ($IC_{50}$=0.04μM), G449P $pIC_{50}$=4.66±0.16 ($IC_{50}$=21.87μM)). The G449P variant also showed a slightly lower enzymatic activity **(Fig. 3D)** (*Pf*CLK3 Vmax=1.24, G449P Vmax=0.88) but higher Km for ATP **(fig. S7A)** (*Pf*CLK3 Km=6.29, G449P Km=81.3) compared to wild type *Pf*CLK3. Single cross over homologous recombination targeting the *Pf*CLK3 locus with a construct designed to insert

the coding sequence for G449P mutant **(Fig. 3E)** generated two independent clones (A3 and A8), which expressed the G449P mutant in place of the wild type *Pf*CLK3 **(Fig. 3F,G)**. Integration of the plasmid at the target locus was verified by PCR of genomic DNA **(Fig. 3F)**, and Western blotting confirmed expression of the G449P mutant which was epitope tagged with a haemaggultinin (HA) tag at the C-terminus **(Fig. 3G). The growth rate of the G449P expressing mutant parasites were not significantly different from control 3D7 parasites (fig. S7B).** Importantly, the activity of TCMDC-135051 in parasite viability assays was seen to be significantly reduced by ~1.5 log units in both clones of G449P **(Fig. 3H)** (the negative logarithm of the half maximal effect ($pEC_{50}$) of TCMDC-135051 in the Dd2 wild type = 6.35 ± 0.038 ($EC_{50}$= 0.45μM) and in the A3 strain = 4.86 ± 0.13 ($EC_{50}$= 13.80μM) and the A8 strain = 4.94 ± 0.051 ($EC_{50}$= 11.48μM)), providing further evidence that TCMDC-135051 kills parasites via inhibition of *Pf*CLK3.

Previous efforts to make inhibitor-insensitive versions of apicomplexan protein kinases have focused on the mutation of the gate keeper residue, a key residue in the ATP binding pocket that can provide steric hindrance to ATP competitive protein kinase inhibitors (*5, 29, 30*). In contrast, our approach was based on a comparison of residues between two highly related kinases (*Pf*CLK1 and *Pf*CLK3) that showed differential sensitivity to an inhibitor. By swapping residues between the kinases we introduced inhibitor in-sensitivity into our target kinase (e.g. *Pf*CLK3) in a strategy that could be applied to other protein kinases.

**Inhibition of *Pf*CLK3 prevents trophozoite to schizont transition**

To characterize the phenotypic response to *Pf*CLK3 inhibition and to understand *Pf*CLK3 function, *P. falciparum* 3D7 parasites synchronised at ring stage (time point zero) were treated with TCMDC-135051 (1μM). The parasites progressed to late ring stage (time point

20 hours) **(Fig. 4A)** but did not progress further to trophozoite stage (time point 30 and 40 hours), arresting with a condensed and shrunken appearance **(Fig. 4A)**. Similar effects were observed if the parasites were treated at mid ring stage (time point 10 hours). Treatment of parasite at later time points (20 hours or 30 hours) blocked development of the parasite from trophozoite to schizont stage. The fact that the parasites at the schizont stage were not viable was further evidenced by the absence of ring stage parasites when the culture was continued to the 50-hour time point **(Fig. 4A)**. These data indicated that *Pf*CLK3 inhibition prevented the transition of the parasites at early (ring to trophozoite) as well as late stages (trophozoite to schizont) of development and importantly did not allow parasites to reach to the next invasion cycle **(Fig. 4A)**. These data further indicated that *Pf*CLK3 inhibition resulted in rapid killing with no evidence that the compound results in quiescence from which the parasite can recover following drug withdrawal. These features were confirmed in parasite reduction rate (PRR) assays, which showed that treatment of parasites with ten fold $EC_{50}$ of TCMDC-135051 completely killed the parasite in 48 hours and viable parasites could not be observed despite maintaining the parasite culture for 28 days following withdrawal of TCMDC-135051 **(Fig. 4B).**

**Inhibition of *Pf*CLK3 disrupts transcription**

Since *Pf*CLK3 has been proposed to regulate RNA processing (*20*) and is closely related to the human kinases PRPF4B and CLK2 that are involved in RNA splicing (*19*) we investigated changes in gene transcription in parent Dd2 parasites and the drug-resistant stain TM051C, in response to exposure to TCMDC-135051. RNA isolated from trophozoite stage parasites was extracted following a short 60 minute treatment with TCMDC-135051 (1μM), a period of time in which the Dd2 and TM051C parasites maintained normal morphology. Genome-

wide transcriptional patterns were determined using oligonucleotide microarray chips that probed 5752 *P. falciparum* genes (*31*). Under these conditions 779 gene transcripts were significantly down-regulated in response to *Pf*CLK3 inhibition in the Dd2 parasites and 155 genes were up-regulated **(Fig 4C, table S2)**. That the majority of these transcriptional changes were due to inhibition of *Pf*CLK3 and not off-target events was supported by the fact that under the same conditions only 6 genes were up-regulated and 88 down-regulated in the resistant TM051C parasite strain **(Fig. 4D, table S3)**. By subtracting the transcriptional changes observed in the TM051C strain, defined here as "off-target", from those observed with the Dd2 parent, the transcriptional changes due to "on-target" inhibition of *Pf*CLK3 were defined **(table S4)**. Among these "on-target" down-regulated genes were those involved in key parasite processes such as egress and invasion, cytoadherence, parasite protein export and involvement in sexual stages as well as house-keeping functions including metabolism, RNA processing, lipid modification and mitochondrial function **(Fig. 4E, table S4)**. Importantly, of the 696 "on-target" genes identified as down-regulated by *Pf*CLK3 inhibition (**table S4)**, 425 matched those that have recently been determined to be essential for asexual *P. falciparum* survival (*12*) **(table S4).**

Gene ontology enrichment analysis was used to determine biological functions that were disproportionally down-regulated by *Pf*CLK3 inhibition. In this analysis, genes associated with key biological functions particularly protein modification, phospholipid biosynthesis and lipid modification were significantly over-represented amongst those genes that were down-regulated **(fig. S8, table S5)**. Importantly, 93% of the "on-target" down-regulated genes contained introns **(Fig. 4F, table S4)**, compared to 52% of genes in the *P. falciparum* genome that are annotated as containing introns(*32*) **(Fig. 4G).** Hence, *Pf*CLK3 inhibition significantly affected

transcription of genes that contained introns ($p < 0.0001$, Pearson chi-squared test), further supporting its role in splicing

**It was of interest that in addition to the nearly 700 genes down-regulated in response to *Pf*CLK3 inhibition there were 154 genes that were significantly up-regulated (table S4). Amongst these were genes associated with RNA processing, such as splicing factor 1 (PF3D7_1321700) and pre-mRNA-splicing factor SYF1 (PF3D7_1235900), indicating that at least some of the up-regulated genes may represent compensatory mechanisms. In support of this notion was the finding that *Pf*CLK3 itself was within the up-regulated genes (table S4).**

**Cross species and *in vivo* activity of TCMDC-135051**

It might be predicted that the close similarity between orthologues of CLK3 in different malaria parasites species would result in TCMDC-135051 showing similar activities against CLK3 from different *Plasmodium* species. This indeed was the case as *in vitro* kinase assays using recombinant *Pv*CLK3 (*P. vivax*) and *Pb*CLK3 (*P. berghei*) (**fig. S9A,B)**, showed that TCMDC-135051 had near equipotent inhibition at these two orthologues with $pIC_{50}$ values of 7.47 ± 0.12 ($IC_{50}$=0.033μM) and 7.86 ± 0.10 ($IC_{50}$=0.013μM) respectively **(fig. S9A,B).** Furthermore, in asexual blood stage cultures of both *P. knowlesi* (an experimental model for *P. vivax*) and *P. berghei* (a rodent malaria model used for *in vivo* drug testing (*33*)), inhibition of *Pf*CLK3 by TCMDC-135051 resulted in parasiticidal activity at both of these *Plasmodium* species **(Fig. 5A,B)**. The potent and efficacious effects of TCMDC-135051 in blood *P. berghei* cultures prompted an investigation of the *in vivo* activity of TCMDC-135051 in mice infected with *P. berghei*. Twice daily intraperitoneal dosing of TCMDC-135051 into mice infected with *P. berghei* resulted in a dose-related reduction in parasitaemia over a 6 day infection period

where the maximal dose (50mg/kg) resulted in near complete clearance of parasites from peripheral blood **(Fig. 5C)**.

**Activity of TCMDC-135051 at liver invasion and sporozoite development**

TCMDC-135051 showed potent activity against *P. berghei* sporozoites in a liver invasion and development assay (*34*) in which the compound showed a $pEC_{50}$ value of 6.17 ± 0.10 ($EC_{50}$=0.40μM) **(fig. S11)**, although hepatocyte toxicity **(fig. S11)** was observed but only significantly at 10μM **(fig. S11)**.

**Targeting *Pf*CLK3 reduces transmission to the mosquito vector**

Effects of PfCLK3 inhibition on sexual stage parasites was tested in an assay developed using the *P. falciparum Pf*2004 parasite strain that shows high levels of gametocyte production (*35*). Importantly, TCMDC-135051 showed potent parasiticidal activity in asexual stage *Pf*2004 **(fig. S12A)** ($pEC_{50}$ in *Pf*2004 = 6.58 ± 0.01 ($EC_{50}$=0.26μM) similar to that seen in asexual 3D7 and Dd2 parasites. In addition, TCMDC-135051 showed inhibitory activity between commitment of infected red blood cells to gametogenesis and stage II gametocytes with a $pEC_{50}$ = 6.04 ± 0.11 ($EC_{50}$=0.91μM) **(fig. S12B).**

These *in vitro* studies were followed by mosquito membrane feeding assays to test directly the impact of *Pf*CLK3 inhibition on transmission of *P. falciparum* to the mosquito vector. In these experiments stage II gametocytes (from 3D7 parasites) were exposed to TCMDC-135051 and allowed to develop to stage V in the continued presence of drug. These experiments showed a concentration-dependent decrease in stage V gametocyte number **(Fig. 5D).** When analysed using a generalised linear mixed model (GLMM) this effect had a potency of $EC_{50}$=0.8μM **(Fig. 5E)**. Furthermore, the inhibition of *Pf*CLK3 significantly

decreased exflagellation (**Fig. 5E,F**; $EC_{50}$=0.2μM), which combined with the effect on gametocyte number contributed to a significant reduction in transmission as measured by the prevalence of oocysts in the gut of mosquitoes in membrane feeding assays **(Fig. 5G,H).**

These studies were further extended to test the effects of *Pf*CLK3 inhibition on stage V gametocytes. **While exposure of stage V gametocytes to TCMDC-135051 for 24 hours did not affect gametocyte number (fig. S13A,B) a small but significant reduction in exflagellation (~25% reduction, $p<2x10^{-16}$ as determined by the GLMM) was observed at the highest concentration tested (fig. S13C,D). A more pronounced effect was observed in membrane feeding experiments where mosquito transmission was significantly reduced by ~50% (fig. S13e,f, $p=4.33x10^{-6}$). A reduction of mosquito infection prevalence of 50% is likely to have a major effect in field conditions where infection rates in mosquitoes are usually <5%.**

**Discussion**

Here we identify *Pf*CLK3 as a valid and druggable anti-malarial target for both sexual and asexual stages of parasite development **including liver stage**. This suggests that targeting *Pf*CLK3 might not only be a novel strategy for developing curative treatments for malaria by clearance of asexual blood stage parasites and as a **potential prophylactic by targeting liver stage** but also the parasiticidal activity afforded by *Pf*CLK3 inhibition at gametocytes would indicate that through this mechanism transmission to the insect vector could also be affected. Since splicing of essential transcripts occurs at many stages of the parasite life cycle it is attractive to hypothesise that inhibition of *Pf*CLK3, which has been implicated in the phosphorylation of splicing factors necessary for the assembly and activity of the spliceosome (*17, 18, 20*), would have a wide-ranging impact on parasite viability. In support

of this notion is the finding that *Pf*CLK3 inhibition down-regulated over 400 essential parasite transcripts. Interestingly, the majority of down-regulated transcripts are from genes that contain introns (91%), providing further evidence that *Pf*CLK3 is involved in RNA splicing and disruption of this essential process at multiple life cycle stages is the likely mechanism by which inhibitors of *Pf*CLK3 have parasiticidal activity.

The similarity of CLK3 orthologues in *Plasmodium sp*. suggests inhibitors might also have activity across a number of *Plasmodium* species. This was confirmed here by almost equipotent inhibition of the kinase activity of *Pv*CLK3, *Pb*CLK3 and *Pf*CLK3 by TCMDC-135051. This *in vitro* action was mirrored by *ex vivo* activity in *P. berghei* and *P. falciparum but also P. knowlesi* (a model for *P. vivax*) indicating that inhibition of *Plasmodium* CLK might have cross species activity. This coupled to the reduction in transmission following *Pf*CLK3 inhibition points to *Pf*CLK3 satisfying many of the criteria set by MMV for a suitable target for next generation anti-malarials; namely a target that can deliver rapid, multi-stage, parasite killing across multiple species with action as a transmission blocker (*36*).

One of the major barriers associated with the development of protein kinase inhibitors is the issue of selectivity since the ATP binding pocket, to which the majority of protein kinase inhibitors bind, is very similar between protein kinases (*37*). Here TCMDC-135051 shows surprising selectivity towards *Pf*CLK3 even when compared to its paralogue in *P. falciparum Pf*CLK1 and the orthologue in human (PRPF4B) and the closely related human kinase CLK2. Furthermore, the fact that our transcriptional studies revealed very few off-target events and that adaptive resistance and chemogenetic resistance was associated with single point mutations in *Pf*CLK3 indicates that the selectivity of TCMDC-135051 for *Pf*CLK3 observed *in vitro* was maintained in the parasite. The fact that a hit from a library screen can show such selectivity against human and parasite kinases provides encouragement that *Pf*CLK3

selective inhibitors can be generated that might provide therapeutic efficacy with low off-target toxicity.

Despite the fact that lipid kinases such as phosphatidylinositol-4 kinase are considered promising targets (*38*) in malaria and the abundant evidence that phosphorylation and phospho-signalling is crucial for the viability of both asexual and sexual stages of the malaria parasite (*5, 8, 10, 11*) together with reports identifying essential parasite protein kinase targets (*8, 11*), and the extensive experience of academic and industrial laboratories in the design of protein kinase inhibitor drugs (*14, 37*), the targeting of parasite protein kinases in anti-malarial drug development is only in its infancy (*6, 39*). By focusing on an essential parasite kinase and taking advantage of high throughput phenotypic screens of commercial and academic libraries (*21, 40, 41*) as a starting point to screen for inhibitors, we have identified a probe molecule that has not only established the validity of *Pf*CLK3 as a target in malaria but also determined that this protein kinase is susceptible to selective pharmacological inhibition by small drug-like molecules. In this way, our study lends weight to the argument that targeting the essential parasite protein kinases identified through global genomic studies might be a valid therapeutic strategy in the development of molecules that meet many of the criteria set for the next generation of anti-malarial drugs.

**Summary of key materials and methods**

***(For full materials and methods see supplementary information)***

**High throughput Screening**

Compounds were tested in single shot at 10 µM, or in dose response from 100 µM (11-point, 3-fold serial dilutions). Screening was performed in 1536-well plates, with final reaction and read-out volumes of 4 µL and 6 µL, respectively. The results from the High-Throughput screening were further analysed using Activity Base (ID Business Solutions Ltd., Surrey, UK). For each test compound, % inhibition was plotted against compound concentration.

**Evolution of compound-resistant lines and whole genome sequencing**

The *P. falciparum* Dd2 strain was cultured in triplicate in the presence of increasing concentrations of TCMDC-135051 to generate resistant mutants as previously described(*42*). After approximately 60 days of selection parasites were cloned in 96-well plates by limiting dilution(*43*). The half maximal (50%) inhibitory concentration was determined in dose-response format using a SYBR Green-I based cell proliferation assay as previously described(*41*). To determine genetic variants that arose during selection genomic DNA was sequenced on an Illumina Mi-seq and single-nulceotide variants were detected using the Genome Analysis Toolkit (GATK v1.6).

**Generation of G449 mutant parasite**

Fragment of *Pf*CLK3 gene containing part of exon2, exon 3, exon 4 and part of exon 5 (1143 bp) corresponding to 655-1797 bp in clk3 genomic sequence was amplified using primer CLK3-HR1 and CLK3-HR2 and the amplified product named as *Pf*CLK3 Homologous region (CLK3-HR) was cloned in pHH1 derived vector using restriction sites HpaI and BglII. The rest of clk3 gene sequence down stream of CLK3-HR corresponding to 1798-3152 bp *Pf*clk3

genomic sequence were modified by removing introns and the stop codon and the coding sequence was optimized for *E.coli* codon usage to make it dis-similar to *Pf*clk3 genomic sequence. This fragment of gene which we named as *Pf*CLK3-codon optimized (CLK3-CO) was commercially synthesized and included BglII recognition site at 5' and XhoI recognition site at 3'. CLK3-CO was cloned downstream of CLK3-HR region in the parent plasmid using BglII and XhoI restriction sites in such a way that the triple HA tag sequence in the parent plasmid remained in frame with the *Pf*clk3 sequence. The BglII restriction site that was artificially introduced for cloning purpose was mutated back to original *Pf*CLK3 coding sequence by site directed mutagenesis using CLK3-BglII-KN1 and CLK3-BglII-KN2 primers. Site directed mutagenesis was used again to mutate Glycine in *Pf*CLK3 at position 449 to an alanine. The targeting vector generated was used for transfection of schizont stage parasites.

**Figure Legends**

**Figure 1. High-throughput screen identifies inhibitors to *Pf*CLK1 and *Pf*CLK3**.

**(A)** Percent Inhibition distribution pattern of compounds screened against *Pf*CLK3, binned in 5% intervals. Active "hit' compounds were defined as those that were positioned > 3SDs from the mean. **(B)** Pie-chart summary of the primary single dose screen. **(C)** Hit compounds were used in concentration response curves. Shown is a comparison of $pIC_{50}$ values for inhibition of *Pf*CLK3 vs *Pf*CLK1. TCMDC-135051 (structure shown) is highlighted as the most potent and selective *Pf*CLK3 hit. **(D)** The same data as shown in c but in pie chart format of compounds designated as inactive, pan-active (activity against both *Pf*CLK1 and *Pf*CLK3), and those selective for either *Pf*CLK1 or *Pf*CLK3.

**Figure 2. Parasites adapted to become less sensitive to TCMDC-135051 harboured mutations in the *pfclk3* gene.**

**(A)** To generate TCMDC-135051 resistant parasite lines Dd2 parasites were cultured with increasing concentrations of TCMDC-135051 over a 2 month period. This protocol resulted in three lines that were less sensitive to TCMDC-135051 but with unchanged sensitivity against artemisinin (ART) and chloroquine (CQ). **(B)** Illustration of the position of the mutations in the *pfclk3* gene and *pfusp39* gene in the drug resistant mutant lines. **(C)** The line showing the greatest change in sensitivity to TCMDC-135051, TM051C, expressed a mutant form of *Pf*CLK3 where histidine 259 was substituted by a proline (illustrated). Shown are death curves for parental and TM051C lines. **(D)** Enzyme activity of recombinant *Pf*CLK3 and the H259P mutant determined at varying ATP concentrations to derive a Km for ATP. **(E)** TCMDC-135051 kinase inhibition curves for *Pf*CLK3 and the H259P mutant at Km ATP

concentrations for each enzyme. Data presented is the mean ± S.E.M of at least 3 independent experiments.

**Figure 3. Chemogenetic validation of *Pf*CLK3 as a target for the parasiticidal activity of TCMDC-135051.**

**(A)** Schematic of the primary amino sequence of *Pf*CLK3 showing the 11 kinase subdomains and the amino acid sequence of subdomain V of *Pf*CLK1 and *Pf*CLK3. **(B)** Gel based assay of the phosphorylation of MBP by *Pf*CLK3 and a variant where glycine at position 449 was substituted for a proline (G449P). The top gel is an autoradiograph and the bottom a Coomassie stain of the same gel. **(C)** TCMDC-135051 inhibition of recombinant *Pf*CLK3 and the G449P mutant. **(D)** Maximal kinase activity of recombinant *Pf*CLK3 compared to the activity of the G449P mutant. **(E)** Schematic of gene targeting strategy that would result in the expression of the G449 mutant (containing a triple HA-tag) in place of wild type *Pf*CLK3. **(F)** The recombination event illustrated in "e" was identified in cloned G449P parasite cultures by PCR (A3 and A8). **(G)** Expression of the triple HA-tagged G449P mutant in genetically engineered parasite cultures (G449P) was determined by Western blotting. Gel on the left probed lysates with anti-HA antibodies, in the middle is a loading control probed with anti-*Pf*CDPK1 antibodies and on the right is a Coomassie stain of the lysate preparations used in the Western blots. **(H)** The growth inhibition curves of TCMDC-135051 against parent 3D7 parasites and G449P parasites (A3 and A8). The data shown in the graphs are the mean ±S.E.M of at least three independent experiments. *$p<0.05$ t-test.

**Figure 4. Inhibition of *Pf*CLK3 prevents trophozoite to schizont transient, kills the parasite with rapid kinetics and disrupts gene transcription**

**(A)** Smears of synchronised blood stage *P. falciparum* cultures following treatment with TCMDC-135051 (2μM) were taken at the indicated times after TCMDC-135051 administration. **(B)** The *in vitro* parasite reduction rate in the presence of 10 x $EC_{50}$ of TCMDC-135051 was used to determine the onset of action and rate of killing. The data presented represents the mean ±S.E.M. Previous results reported on standard anti-malarials tested at 10 × $EC_{50}$ using the same conditions are shown for comparison (*44*). **(C,D)** Illustration of the genes that are designated as significantly changing (Moderate t test n=4) in transcription following treatment with TCMDC-135051 (1μM, 60 mins) of either **(c)** parent Dd2 parasites or **(D)** TM051C mutant parasites. Each line represents the log2 fold change in the probes used in the micro-array. The number of genes represented by the probes are indicated. **(E)** Summary of the parasite processes associated with the genes where transcription is significantly down-regulated following TCMDC-135051 treatment. **(F)** Assessment of intron containing genes among genes that are up-regulated and down-regulated in Dd2 parasites following TCMDC-135051 treatment. **(G)** Assessment of intron containing genes in the plasmodium genome (data derived from Plasmodb).

**Figure 5. Inhibition of *Pf*CLK3 has parasiticidal activity at multiple parasite species, shows *in vivo* parasiticidal activity in *P. berghei*, blocks gametocyte development and reduces transmission to the mosquito vector.**

Concentration effect curve of TCMDC-135051 on blood stage **(A)** *P. knowlesi* and **(B)** *P. berghei* parasites. **(C)** TCMDC-135051 *P. berghei in vivo* growth inhibition curves and Day 4 percentage suppression plots (insert). Error bars are standard deviations from n=4 mice

groups. Statistical comparisons between drug treated and vehicle are shown using the one way ANOVA and Dunnett's multiple comparisons test. **** p <0.0001. **(D-H)** Concentration-effect of exposure of stage II-V *P. falciparum* (clone 3D7) gametocytes to TCDMDC-135051 on **(D,E)** gametocyte (GC) numbers in culture, **(E,F)** exflagellation, and **(G,H)** prevalence (number of mosquitoes with oocyst infection / number of mosquitoes dissected)

of infection of *An. coluzzii* mosquitoes. Graphs **(D,E,F)** show the mean ±SEM of 4 independent experiments. Panels **(E,F,H)** show the predicted effects of drug concentrations according to the maximal GLMM with the shaded area indicating 95% confidence intervals. From the GLMM analysis the approximate $EC_{50}$ values were calculated.

**Table 1: Adaptive resistance to TCMDC-135051.** Dd2 parasites were exposed to sub-threshold concentrations of TMDC-135051 and three lines isolated that were less sensitive to TCMDC-135051 but with unchanged sensitivity to artemisinin (ART) and chloroquine (CQ). Shown are nucleotide changes and associated amino acid changes in genes from the resistance lines as well as the identity and annotated function of the mutant genes. $IC_{50}$ values associated with each line for ART, CQ and TCMDC-135051 together with the fold change in $IC_{50}$ for TCMDC-135051 compared to Dd2 parent parasites are shown. Data is the mean ± S.E.M of three experiments.

**References**


1. J. Straimer *et al.*, Drug resistance. K13-propeller mutations confer artemisinin resistance in Plasmodium falciparum clinical isolates. *Science* **347**, 428-431 (2015).
2. F. Ariey *et al.*, A molecular marker of artemisinin-resistant Plasmodium falciparum malaria. *Nature* **505**, 50-55 (2014).
3. C. Amaratunga *et al.*, Dihydroartemisinin-piperaquine resistance in Plasmodium falciparum malaria in Cambodia: a multisite prospective cohort study. *Lancet Infect Dis* **16**, 357-365 (2016).
4. R. Leang *et al.*, Evidence of Plasmodium falciparum Malaria Multidrug Resistance to Artemisinin and Piperaquine in Western Cambodia: Dihydroartemisinin-Piperaquine Open-Label Multicenter Clinical Assessment. *Antimicrob Agents Chemother* **59**, 4719-4726 (2015).
5. M. M. Alam *et al.*, Phosphoproteomics reveals malaria parasite Protein Kinase G as a signalling hub regulating egress and invasion. *Nature communications* **6**, 7285 (2015).
6. C. Doerig, J. C. Rayner, A. Scherf, A. B. Tobin, Post-translational protein modifications in malaria parasites. *Nature reviews. Microbiology* **13**, 160-172 (2015).
7. E. Lasonder, M. Treeck, M. Alam, A. B. Tobin, Insights into the Plasmodium falciparum schizont phospho-proteome. *Microbes and infection / Institut Pasteur* **14**, 811-819 (2012).
8. L. Solyakov *et al.*, Global kinomic and phospho-proteomic analyses of the human malaria parasite Plasmodium falciparum. *Nature communications* **2**, 565 (2011).
9. C. Doerig *et al.*, Protein kinases of malaria parasites: an update. *Trends Parasitol* **24**, 570-577 (2008).
10. E. Bushell *et al.*, Functional Profiling of a Plasmodium Genome Reveals an Abundance of Essential Genes. *Cell* **170**, 260-272 e268 (2017).
11. R. Tewari *et al.*, The systematic functional analysis of Plasmodium protein kinases identifies essential regulators of mosquito transmission. *Cell host & microbe* **8**, 377-387 (2010).
12. M. Zhang *et al.*, Uncovering the essential genes of the human malaria parasite Plasmodium falciparum by saturation mutagenesis. *Science* **360**, eaap7847 (2018).
13. S. Gross, R. Rahal, N. Stransky, C. Lengauer, K. P. Hoeflich, Targeting cancer with kinase inhibitors. *J Clin Invest* **125**, 1780-1789 (2015).
14. L. N. Johnson, Protein kinase inhibitors: contributions from structure to clinical compounds. *Q Rev Biophys* **42**, 1-40 (2009).
15. C. Doerig *et al.*, Malaria: targeting parasite and host cell kinomes. *Biochimica et biophysica acta* **1804**, 604-612 (2010).
16. Z. Zhou, X. D. Fu, Regulation of splicing by SR proteins and SR protein-specific kinases. *Chromosoma* **122**, 191-207 (2013).
17. S. Agarwal *et al.*, Two nucleus-localized CDK-like kinases with crucial roles for malaria parasite erythrocytic replication are involved in phosphorylation of splicing factor. *J Cell Biochem* **112**, 1295-1310 (2011).
18. E. Talevich, A. Mirza, N. Kannan, Structural and evolutionary divergence of eukaryotic protein kinases in Apicomplexa. *BMC Evol Biol* **11**, 321 (2011).
19. M. Schneider *et al.*, Human PRP4 kinase is required for stable tri-snRNP association during spliceosomal B complex formation. *Nat Struct Mol Biol* **17**, 216-221 (2010).

20. S. Kern *et al.*, Inhibition of the SR protein-phosphorylating CLK kinases of Plasmodium falciparum impairs blood stage replication and malaria transmission. *PloS one* **9**, e105732 (2014).
21. F. J. Gamo *et al.*, Thousands of chemical starting points for antimalarial lead identification. *Nature* **465**, 305-310 (2010).
22. P. Dranchak *et al.*, Profile of the GSK published protein kinase inhibitor set across ATP-dependent and-independent luciferases: implications for reporter-gene assays. *PloS one* **8**, e57888 (2013).
23. R. Axel, Scents and sensibility: a molecular logic of olfactory perception (Nobel lecture). *Angewandte Chemie* **44**, 6110-6127 (2005).
24. T. Spangenberg *et al.*, The open access malaria box: a drug discovery catalyst for neglected diseases. *PloS one* **8**, e62906 (2013).
25. Q. Gao *et al.*, Evaluation of cancer dependence and druggability of PRP4 kinase using cellular, biochemical, and structural approaches. *The Journal of biological chemistry* **288**, 30125-30138 (2013).
26. J. M. Fraile *et al.*, USP39 Deubiquitinase Is Essential for KRAS Oncogene-driven Cancer. *The Journal of biological chemistry* **292**, 4164-4175 (2017).
27. H. Hadjivassiliou, O. S. Rosenberg, C. Guthrie, The crystal structure of S. cerevisiae Sad1, a catalytically inactive deubiquitinase that is broadly required for pre-mRNA splicing. *RNA* **20**, 656-669 (2014).
28. O. V. Makarova, E. M. Makarov, R. Luhrmann, The 65 and 110 kDa SR-related proteins of the U4/U6.U5 tri-snRNP are essential for the assembly of mature spliceosomes. *The EMBO journal* **20**, 2553-2563 (2001).
29. R. Hui, M. El Bakkouri, L. D. Sibley, Designing selective inhibitors for calcium-dependent protein kinases in apicomplexans. *Trends Pharmacol Sci* **36**, 452-460 (2015).
30. S. Lourido *et al.*, Calcium-dependent protein kinase 1 is an essential regulator of exocytosis in Toxoplasma. *Nature* **465**, 359-362 (2010).
31. B. F. Kafsack, H. J. Painter, M. Llinas, New Agilent platform DNA microarrays for transcriptome analysis of Plasmodium falciparum and Plasmodium berghei for the malaria research community. *Malaria journal* **11**, 187 (2012).
32. M. J. Gardner *et al.*, Genome sequence of the human malaria parasite Plasmodium falciparum. *Nature* **419**, 498-511 (2002).
33. D. A. Fidock, P. J. Rosenthal, S. L. Croft, R. Brun, S. Nwaka, Antimalarial drug discovery: efficacy models for compound screening. *Nat Rev Drug Discov* **3**, 509-520 (2004).
34. J. Swann *et al.*, High-Throughput Luciferase-Based Assay for the Discovery of Therapeutics That Prevent Malaria. *ACS Infect Dis* **2**, 281-293 (2016).
35. N. M. Brancucci, I. Goldowitz, K. Buchholz, K. Werling, M. Marti, An assay to probe Plasmodium falciparum growth, transmission stage formation and early gametocyte development. *Nat Protoc* **10**, 1131-1142 (2015).
36. J. N. Burrows *et al.*, New developments in anti-malarial target candidate and product profiles. *Malaria journal* **16**, 26 (2017).
37. R. Roskoski, Jr., A historical overview of protein kinases and their targeted small molecule inhibitors. *Pharmacol Res* **100**, 1-23 (2015).
38. C. W. McNamara *et al.*, Targeting Plasmodium PI(4)K to eliminate malaria. *Nature* **504**, 248-253 (2013).

39. I. S. Lucet, A. Tobin, D. Drewry, A. F. Wilks, C. Doerig, Plasmodium kinases as targets for new-generation antimalarials. *Future medicinal chemistry* **4**, 2295-2310 (2012).
40. W. A. Guiguemde *et al.*, Chemical genetics of Plasmodium falciparum. *Nature* **465**, 311-315 (2010).
41. D. Plouffe *et al.*, In silico activity profiling reveals the mechanism of action of antimalarials discovered in a high-throughput screen. *Proceedings of the National Academy of Sciences of the United States of America* **105**, 9059-9064 (2008).
42. M. Rottmann *et al.*, Spiroindolones, a potent compound class for the treatment of malaria. *Science* **329**, 1175-1180 (2010).
43. I. D. Goodyer, T. F. Taraschi, Plasmodium falciparum: a simple, rapid method for detecting parasite clones in microtiter plates. *Exp Parasitol* **86**, 158-160 (1997).
44. L. M. Sanz *et al.*, P. falciparum in vitro killing rates allow to discriminate between different antimalarial mode-of-action. *PloS one* **7**, e30949 (2012).
45. M. J. Manary *et al.*, Identification of pathogen genomic variants through an integrated pipeline. *BMC bioinformatics* **15**, 63 (2014).

45. C. R. Collins *et al.*, Robust inducible Cre recombinase activity in the human malaria parasite Plasmodium falciparum enables efficient gene deletion within a single asexual erythrocytic growth cycle. *Molecular microbiology* **88**, 687-701 (2013).
46. N. M. B. Brancucci *et al.*, Lysophosphatidylcholine Regulates Sexual Stage Differentiation in the Human Malaria Parasite Plasmodium falciparum. *Cell* **171**, 1532-1544 e1515 (2017).
47. R. Carter, L. Ranford-Cartwright, P. Alano, The culture and preparation of gametocytes of Plasmodium falciparum for immunochemical, molecular, and mosquito infectivity studies. *Methods in molecular biology* **21**, 67-88 (1993).
48. D. Bates, M. Maechler, B. Bolker, S. Walker, Fitting Linear Mixed-Effects Models Using lme4. *Journal of Statistical Software* **67**, 1-48 (2015).
49. R. C. Team. (R Foundation for Statistical Computing, Vienna, Austria., 2017).
50. K. P. Burnham, D. R. Anderson, K. P. Huyvaert, AIC model selection and multimodel inference in behavioral ecology: some background, observations, and comparisons. *Behavioural Ecology and Sociobiology* **65**, 23-35 (2011).
51. S. Nakagawa, P. C. D. Johnson, H. Schielzeth, The coefficient of determination R-2 and intra-class correlation coefficient from generalized linear mixed-effects models revisited and expanded. *J R Soc Interface* **14**, (2017).

Fig. 1

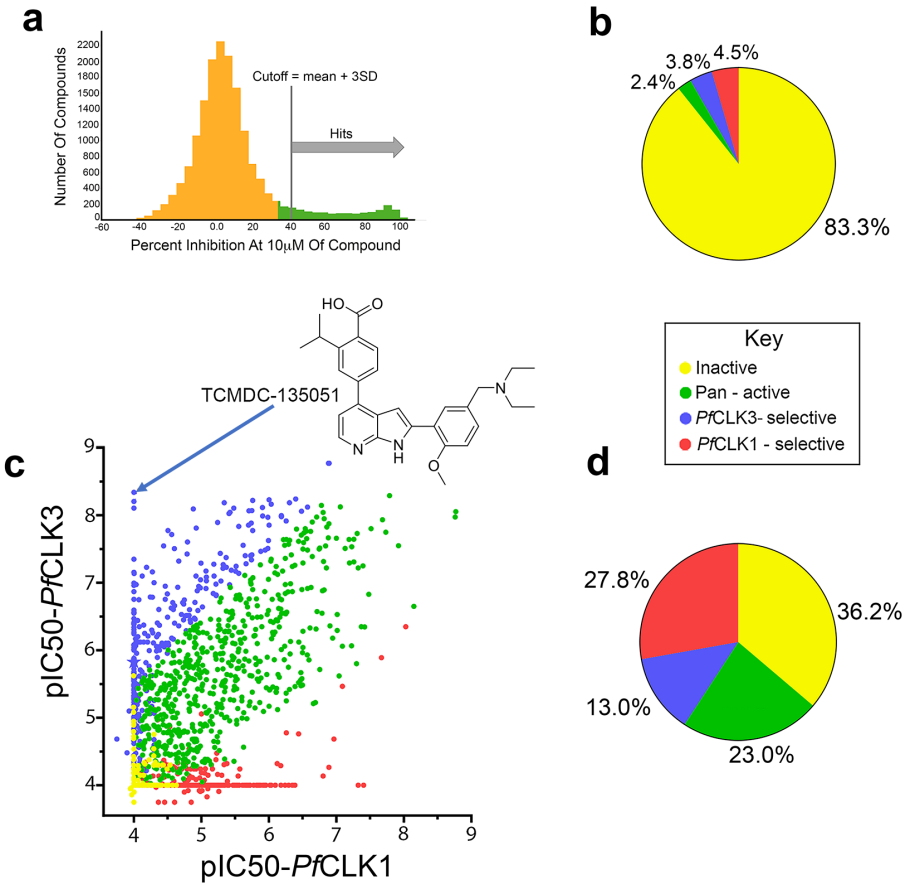
a
Number Of Compounds
Cutoff = mean + 3SD
Hits
Percent Inhibition At 10μM Of Compound
b
3.8%
4.5%
2.4%
83.3%
c
TCMDC-135051
HO
O
N
N
H
O
pIC50-PfCLK3
pIC50-PfCLK1
d
Key
Inactive
Pan - active
PfCLK3- selective
PfCLK1 - selective
27.8%
36.2%
13.0%
23.0%

Fig. 2

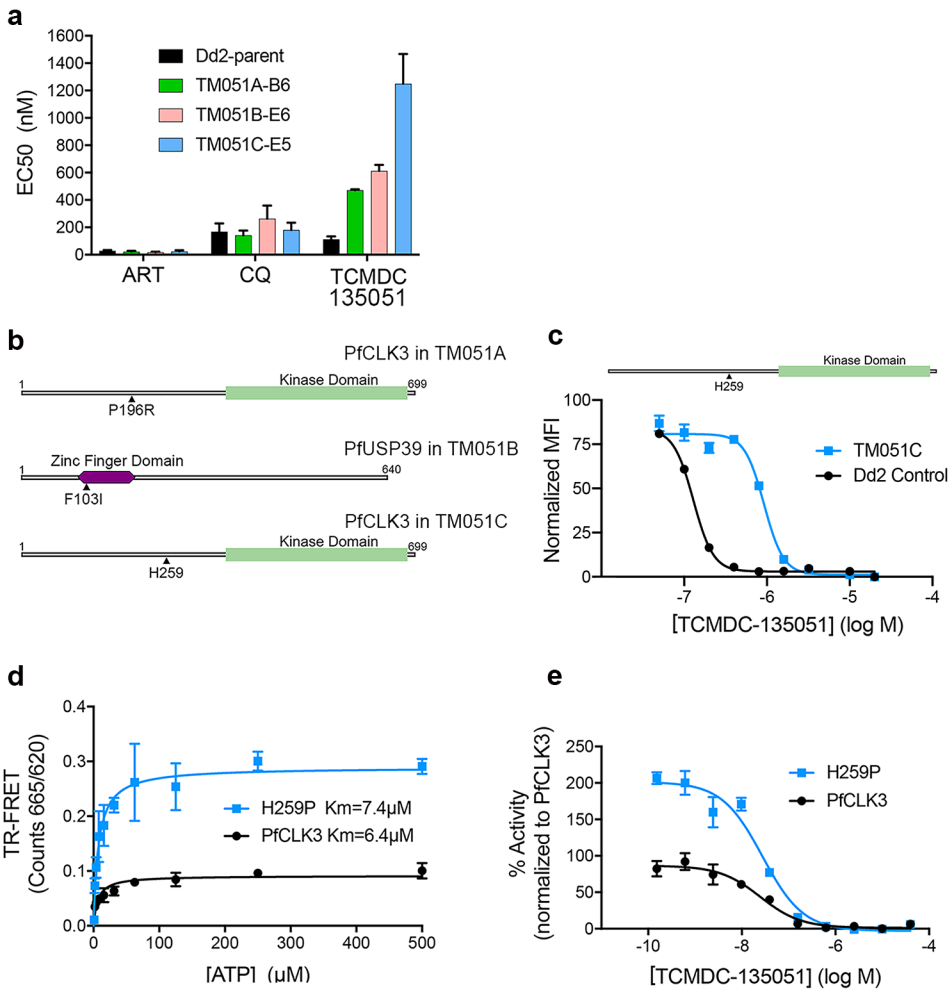
a
EC50 (nM)
Dd2-parent
TM051A-B6
TM051B-E6
TM051C-E5
ART
CQ
TCMDC 135051
b
PfCLK3 in TM051A
Kinase Domain
P196R
PfUSP39 in TM051B
Zinc Finger Domain
F103I
PfCLK3 in TM051C
Kinase Domain
H259
c
Kinase Domain
H259
Normalized MFI
TM051C
Dd2 Control
[TCMDC-135051] (log M)
d
TR-FRET (Counts 665/620)
H259P Km=7.4μM
PfCLK3 Km=6.4μM
[ATP] (μM)
e
% Activity (normalized to PfCLK3)
H259P
PfCLK3
[TCMDC-135051] (log M)

Fig. 3

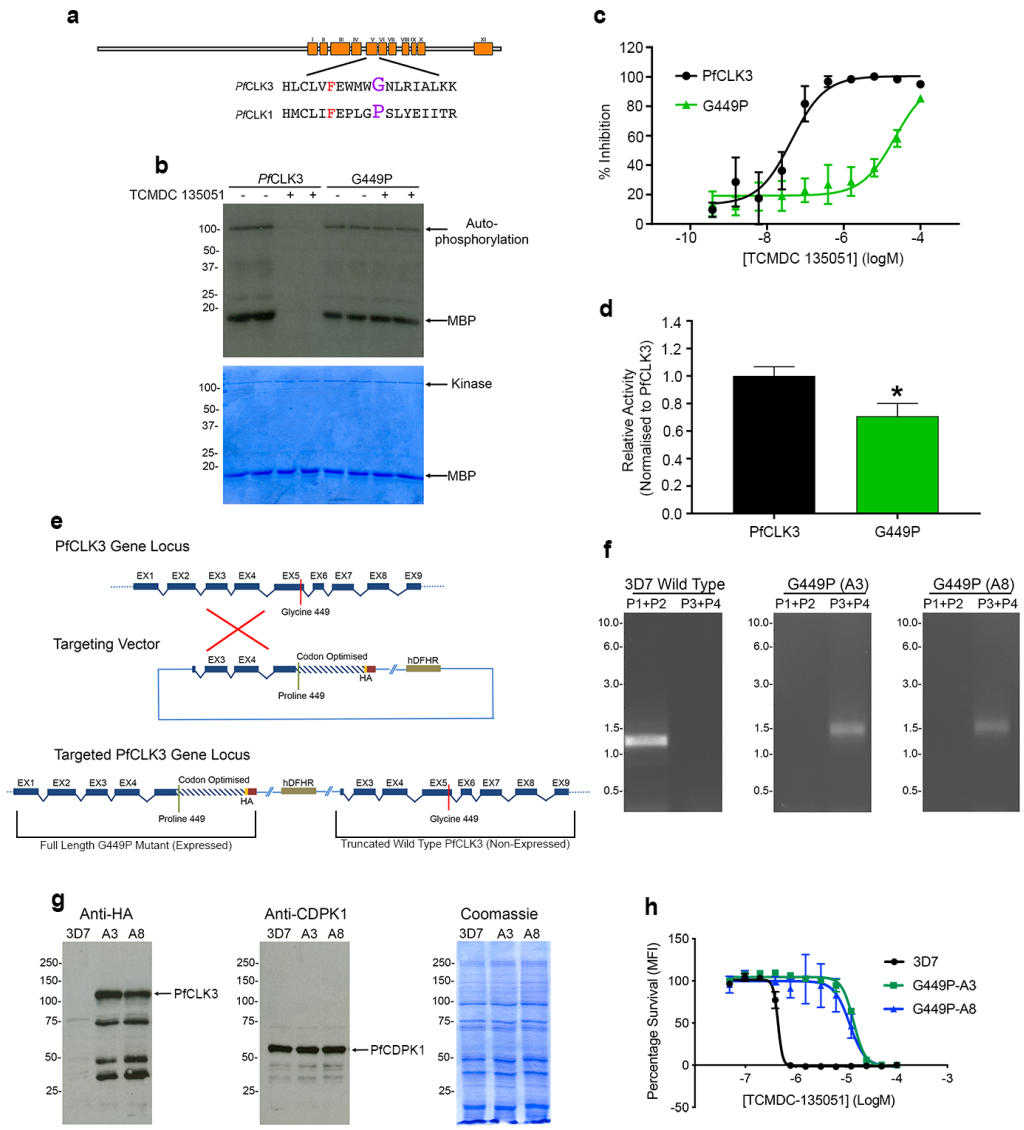
a
PfCLK3 HLCLVFEWMWGNLRIALKK
PfCLK1 HMCLIFEPLGPSLYEIITR
b
PfCLK3
G449P
TCMDC 135051
Auto-phosphorylation
MBP
Kinase
MBP
c
PfCLK3
G449P
% Inhibition
[TCMDC 135051] (logM)
d
Relative Activity (Normalised to PfCLK3)
PfCLK3
G449P
e
PfCLK3 Gene Locus
Glycine 449
Targeting Vector
Codon Optimised
hDFHR
HA
Proline 449
Targeted PfCLK3 Gene Locus
Proline 449
Glycine 449
Full Length G449P Mutant (Expressed)
Truncated Wild Type PfCLK3 (Non-Expressed)
f
3D7 Wild Type
G449P (A3)
G449P (A8)
P1+P2
P3+P4
g
Anti-HA
Anti-CDPK1
Coomassie
3D7 A3 A8
PfCLK3
PfCDPK1
h
Percentage Survival (MFI)
[TCMDC-135051] (LogM)
3D7
G449P-A3
G449P-A8

Fig. 4

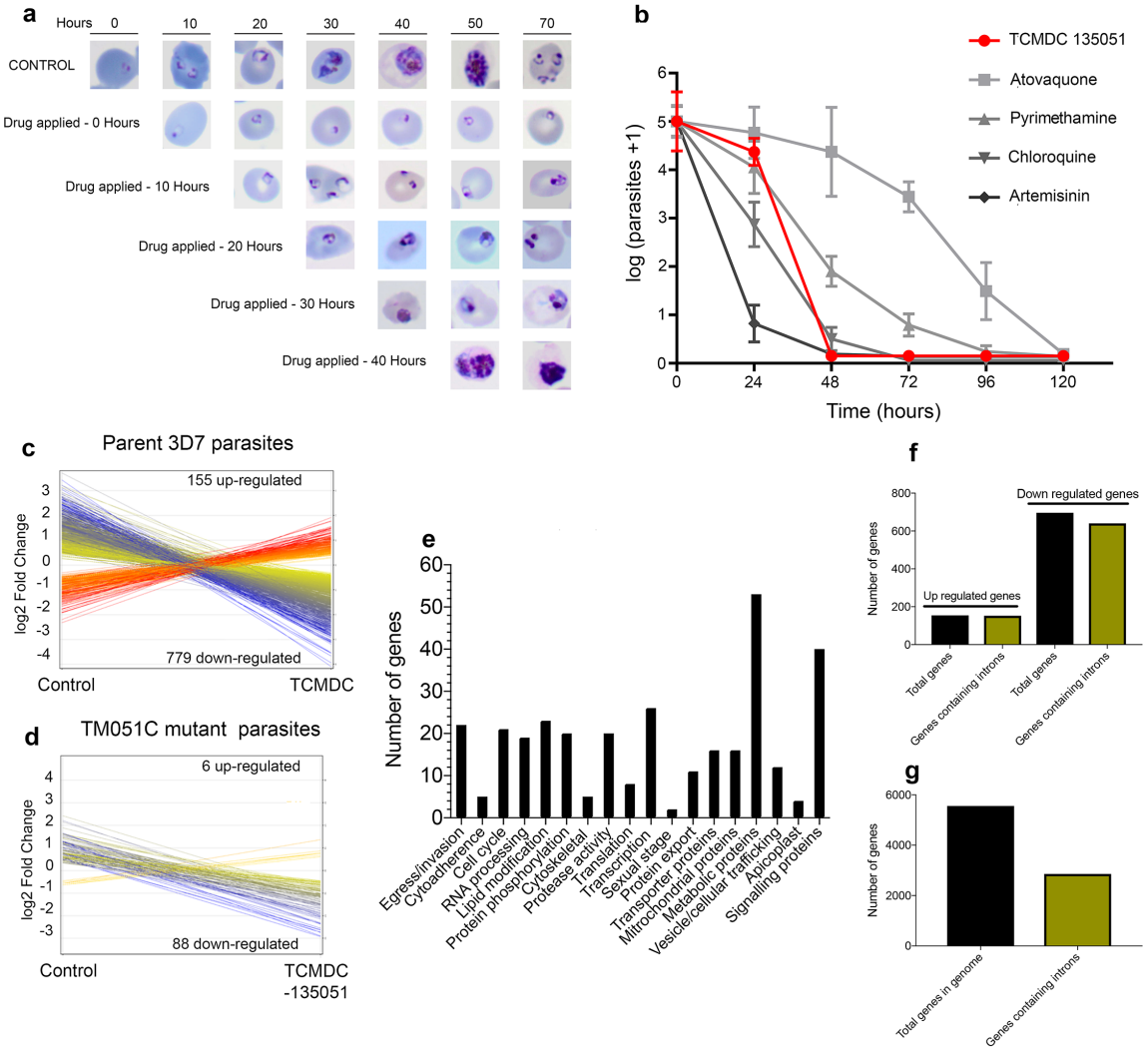
a
Hours 0 10 20 30 40 50 70
CONTROL
Drug applied - 0 Hours
Drug applied - 10 Hours
Drug applied - 20 Hours
Drug applied - 30 Hours
Drug applied - 40 Hours
b
TCMDC 135051
Atovaquone
Pyrimethamine
Chloroquine
Artemisinin
log (parasites +1)
Time (hours)
c
Parent 3D7 parasites
155 up-regulated
779 down-regulated
log2 Fold Change
Control
TCMDC
d
TM051C mutant parasites
6 up-regulated
88 down-regulated
log2 Fold Change
Control
TCMDC -135051
e
Number of genes
Egress/Invasion
Cytoadherence
Cell cycle
RNA processing
Lipid modification
Protein phosphorylation
Cytoskeletal
Protease activity
Translation
Transcription
Sexual stage
Protein export
Transporter proteins
Mitrochondrial proteins
Metabolic proteins
Vesicle/cellular trafficking
Apicoplast
Signalling proteins
f
Number of genes
Down regulated genes
Up regulated genes
Total genes
Genes containing introns
Total genes
Genes containing introns
g
Number of genes
Total genes in genome
Genes containing introns

Fig. 5

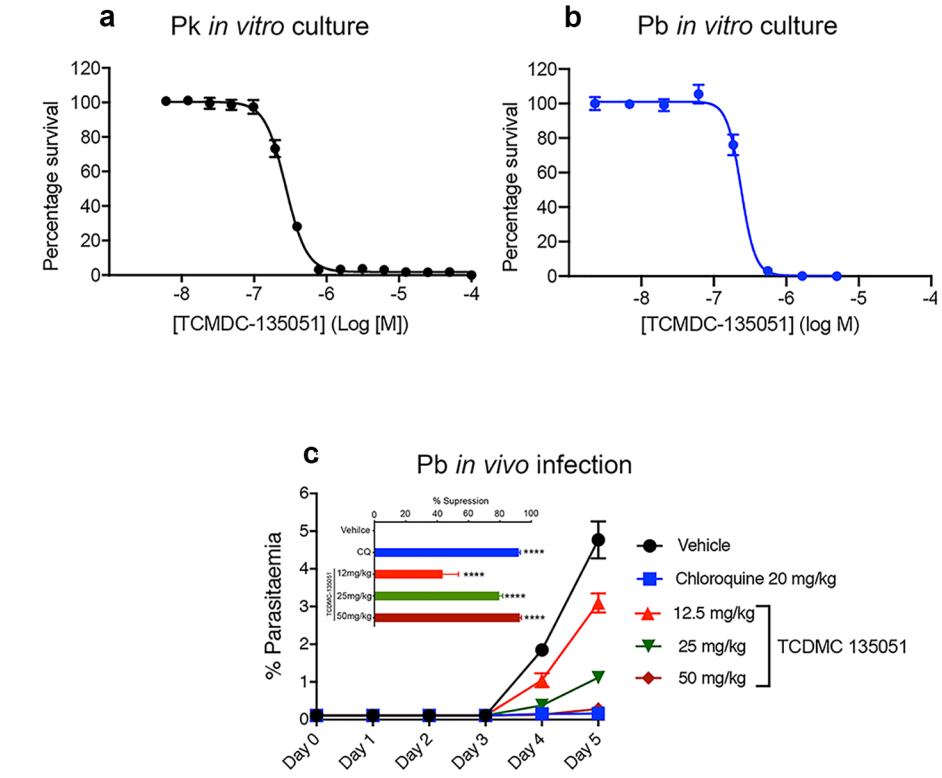
a
Pk *in vitro* culture
Percentage survival
[TCMDC-135051] (Log [M])
b
Pb *in vitro* culture
Percentage survival
[TCMDC-135051] (log M)
c
Pb *in vivo* infection
% Parasitaemia
% Supression
Vehilce
CQ
12mg/kg
25mg/kg
50mg/kg
TCDMC 135051
Vehicle
Chloroquine 20 mg/kg
12.5 mg/kg
25 mg/kg
50 mg/kg
Day 0
Day 1
Day 2
Day 3
Day 4
Day 5

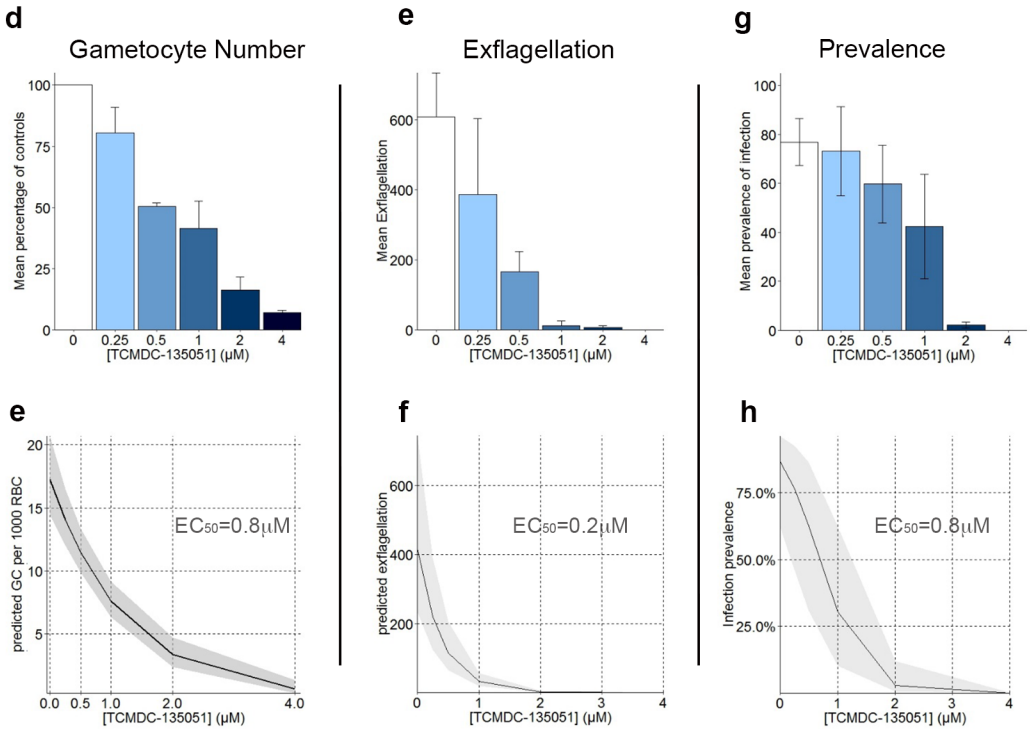
d
Gametocyte Number
Mean percentage of controls
[TCMDC-135051] (μM)
e
Exflagellation
Mean Exflagellation
[TCMDC-135051] (μM)
g
Prevalence
Mean prevalence of infection
[TCMDC-135051] (μM)
e
predicted GC per 1000 RBC
EC50=0.8μM
[TCMDC-135051] (μM)
f
predicted exflagellation
EC50=0.2μM
[TCMDC-135051] (μM)
h
Infection prevalence
EC50=0.8μM
[TCMDC-135051] (μM)

Table 1

| Line | Chr | Position (Mutation) | Mutation | Gene | Annotation | ART (μ M) | CQ (μ M) | TCMDC-135051 (μ M) | Fold Change |
|---|---|---|---|---|---|---|---|---|---|
| Dd2-parent | | | | | | 0.028 ± 0.006 | 0.169 ± 0.059 | 0.113 ± 0.021 | |
| TM051A | 11 | 556351 (C-G) | P196R | Pf3D7_1114700 | CLK3 | 0.022 ± 0.006 | 0.142 ± 0.034 | 0.471 ± 0.007 | 4.2 |
| TM051B | 13 | 708652 (T-A) | F103I | Pf3D7_1317000 | U4/U6.U5 tri-snRNP-associated protein (USP39) | 0.018 ± 0.004 | 0.263 ± 0.096 | 0.613 ± 0.044 | 5.4 |
| TM051C | 11 | 556540 (A-C) | H259P | Pf3D7_1114700 | CLK3 | 0.023 ± 0.010 | 0.180 ± 0.054 | 1.25 ± 0.217 | 11.1 |

**Supplementary Materials:**
Materials and methods
Figures S1-S13
Figure Legends S1-S13
Table Legends S1-S5
Tables (in separate excel files S1-S5)
References 45-51

**Acknowledgments:**

We wish to thank the Proteomics facility of LaCTAD (Laboratório Central de Tecnologias de Alto Desempenho em Ciências da Vida, UNICAMP, Campinas, Brazil), André da Silva Santiago, Angela Maria Fala and Priscila Zonzini Ramos for assistance with PRPF4B protein production and Aché Laboratórios Farmacêuticos for provision of compound A. We wish to thank Elizabeth Peat and Dorothy Armstrong for the maintenance of the IBAHCM/Glasgow University mosquito insectaries, The Scottish National Blood Transfusion service for the provision of human blood and serum, Noushin Emami (Stockholm University) for assistance with serum supplies, and Paul Johnson (IBAHCM, University of Glasgow) for discussions on GLMM. We also thank Professor Rita Tewari for providing *P. berghei* cDNA library. **Funding:** This work has been funded through an MRC Toxicology Unit programme grant (ABT, MMA), MRC Developmental Gap Fund (ASA), Lord Kelvin Adam Smith Fellowship (MMA), GSK Open Lab Foundation Award (ASA), joint MRC Toxicology Unit and MRC Unit the Gambia PhD programme (OJ), Daphne Jackson Fellowship (DM). EAW is supported by grants from the NIH (5R01AI090141 and R01AI103058) and by grants from the Bill & Melinda Gates Foundation (OPP1086217, OPP1141300) as well as by Medicines for Malaria Venture (MMV). Drug WR99210 for selection of transgenic parasites were gifted by Jacobus Pharmaceuticals. MM is supported through WT award 172862-01 and a Wolfson Merit

award from the Royal Society. The Structural Genomics Consortium (SGC) is a registered charity (number 1097737) that receives funds from AbbVie, Bayer Pharma AG, Boehringer Ingelheim, the Canada Foundation for Innovation, the Eshelman Institute for Innovation, Genome Canada, the Innovative Medicines Initiative (European Union [EU]/European Federation of Pharmaceutical Industries and Associations [EFPIA]) (ULTRA-DD grant no. 115766), Janssen, Merck & Company, Merck KGaA, Novartis Pharma AG, the Ontario Ministry of Economic Development and Innovation, Pfizer, the São Paulo Research Foundation (FAPESP number 2013/50724-5), Takeda, and the Wellcome Trust (106169/ZZ14/Z). AC was supported by a Scottish Funding Council Global Challenges Research Fund award to LRC. **Author Contributions:** ABT: conceived the project, designed experiments, analysed data and was the primary author. MMA, ASA, OJ, LCRC: designed experiments, conducted experiments, analysed data and contributed to writing. ELF, AM, KM, ABC, DS, NB, SBM, YAK, NVS, JA, DM, LS, KD, CJ, CZ, MJV, GC, MJL, MLL,: conducted experiments. KC: conducted data analysis. PHCG, JME, DC, DCN, APW, AGJ, LEFA, MM, EAW FJG: contributed to experimental designed and writing the manuscript. . **Competing interests:** The authors declare no conflicts of interest. **Data and materials availability:** all data are available in the manuscript or the supplementary material.

Footnote: Some of the data in this manuscript has been deposited in the not for profit bioarchive (bioRxiv) https://www.biorxiv.org/content/10.1101/404459v1.article-info

**Summary**

**Introduction**

Despite the positive effects of intervention strategies that include insecticide impregnated bed nets and artemisinin-based drug therapies malaria still kills nearly 0.5 million people a year and infects over 200 million individuals globally. This together with the emerging resistance of the parasite to frontline anti-malarials means that there is an urgent need for novel treatments that not only offer a cure for malaria but that also prevent transmission. Here we show that by inhibition of an essential protein kinase that is a key regulator of RNA processing we are able to kill the parasite in the blood and liver stages as well as prevent the development of the sexual stage gametocytes thereby blocking transmission to the mosquito.

**Rationale**

Our group have previously published a list of 36 protein kinases that are essential for blood stage survival of the most virulent form of the human malaria parasite, *Plasmodium falciparum.* Here we focus on one of these protein kinases, PfCLK3, and reason that inhibition of this protein kinase by a small drug-like molecule would be effective at killing blood stage parasites. We further hypothesised that since PfCLK3 plays a key role in RNA splicing that inhibition of this kinase would be effective at killing the parasite all stages of the life cycle where RNA splicing is required. This would include blood, liver and sexual stages.

**Results**

By screening a focused library of nearly 30,000 compounds we identified a probe molecule that selectively inhibited PfCLK3 and that killed blood stage *P. falciparum*. Using a

combination of evolved resistance and chemogenetics we established that our probe molecule had parasiticidal activity by inhibition of PfCLK3. We further demonstrated that inhibition of PfCLK3 in parasites resulted in a reduction in over 400 gene transcripts known to be essential for parasite survival. The fact that the vast majority of the genes down-regulated by PfCLK3 inhibition contained introns supported the notion that inhibition of PfCLK3 killed the malaria parasite by preventing the splicing of essential parasite genes. Since there is a high degree of homology between orthologues of CLK3 in other Plasmodium species (*Plasmodium spp*) it might be expected that our probe molecule would both inhibit CLK contained in other malaria parasite species and have effective parasiticidal activity in these parasites. This was indeed found to be the case with our molecule showing potent inhibition of CLK3 from *P. vivax* and *P. berghei* as well as killing the blood stages of *P. berghei* and *P. knowlesi*. Finally, we demonstrated that PfCLK3 inhibition also kills liver stage *P. falciparum* parasites and importantly prevents the development of gametocytes thereby blocking the infection of mosquitoes.

**Conclusion**

We show that inhibition of the essential malaria protein kinase CLK3 can kill multiple species of malaria parasites at the blood stage as wells as killing liver stage *P. falciparum* and blocking transmission of the parasite to the mosquitoes by preventing gametocyte development. In this way we validate *Plasmodium spp* CLK3 as a target that can offer prophylactic, curative and transmission blocking potential.

**Caption for cover figure**

**A new drug target for malaria.** Inhibition of the malaria parasite protein kinase, PfCLK3, kills blood stage parasites and stops the parasite infecting mosquitoes. In this way PfCLK3 is validated as a curative and transmission blocking drug target in malaria. Shown is an infected human red blood cell under control conditions (left) and where PfCLK3 has been inhibited (right) by the selective PfCLK3 inhibitor shown.

**Supplementary Information**

## Supplementary Materials and Methods

### In vitro Kinase Activities and Inhibition Assay

Kinase assays were carried in kinase buffer containing (20 mM HEPES, pH 7.4, 10 mM $MgCl_2$, 1 mM DTT, 50 μM adenosine triphosphate (ATP), 0.1 MBq [γ-$^{32}$P]-ATP) using 0.5 μg purified His-tagged recombinant protein kinases. Protein kinases were incubated with exogenous substrate, Histone Type IIA 2 μg; Myelin Basic Protein (MBP) 2 μg; and α-Casein 2 μg; or with a PBS as a negative control for 30 minutes at 37°C.

The reactions were stopped by adding equal volume of 2X Laemmli buffer after incubation and boiled for 2 minutes at 60°C. Samples were separated on 15% SDS-PAGE, stained with Coomassie Brilliant Blue and dried by means of vacuum gel drying. Dried gels were exposed to X-ray film at -80°C and autoradiographs were collected.

For *in vitro* inhibition assays, compounds (e.g. TCMDC-135051) was added to a final concentration as indicated. For control, a no inhibitor reaction tube was setup to exclude any other unknown inhibitory effect. All other reaction conditions remained the same. Quantification of activity was carried out using ImageJ (1.49v).

### Time Resolve Florescence Energy Transfer (TR-FRET)

Biochemical kinase assays were carried out using time-resolved florescence energy transfer (TR-FRET) to determine kinase activity, Km for ATP and $IC_{50}$ values for the respective kinases used. TR-FRET reactions were performed using the appropriate amount of kinase (5nM for *Pf*CLK1 and 50 nM for *Pf*CLK3 and G449P) in a kinase buffer (containing 50 mM HEPES, 10

mM $MgCl_2$, 2 mM DTT, 0.1% Tween-20, and 1 mM EGTA), U*Light*-labeled peptide substrate (MBP peptide or CREPtide) and an appropriate europium-labeled anti-phospho antibody in two steps.

First, in a 10 μL reaction volume 5 μL of 2X-required enzyme concentration and 5μL of 2X-required substrate mix and cold ATP were incubated in a 384 well plate at 37°C for 1 hour. Second, following incubation, adding 30 mM EDTA in 1X Lance detection buffer containing 3nM Europium-labeled anti-phospho specific antibody incubated at room temperature for 1-hour to stop the reaction and enhance detection and this is then read using the ClarioStar.

Kinase substrate phosphorylation results in the Europium-labeled anti-phospho specific antibody recognizing the phosphorylated site on the substrate. The Europium donor fluorophore is excited at 320 or 340 nm and energy is transferred to the U*Light* acceptor dye on the substrate, which finally results in the emission of light at 665 nm. The level of ULight peptide phosphorylation determines the intensity of the emission.

To test for inhibition by small molecules such as TCMDC-135051, serial dilution of the inhibitor (made at 4 times the required concentration) was made and added to the protein mixture before adding the substrate mix at 4X the required concentration. For normalization, a no kinase and a no inhibitor reaction wells were included and all experiments were run in triplicate.

**Expression and purification of *Pf*CLKs, *Pf*CDPK1 and *Pf*PKG**

Gene encoding the kinase domain of *Pf*CLK1 (residues 534-857) was amplified using *P. falciparum* (3D7) genomic DNA primers CLK1-FamB1 and CLK1-FamB2 . The amplified product was cloned in plasmid pLEICS-05 (University of Leicester) as has been previously

described for cloning of *Pf*CLK3 (*5*). Plasmids encoding the kinase domain of *Pf*CLK1 (pLEICS-05_*Pf*CLK1 (residues 534-875-5xHIS)) and full length *Pf*CLK3 (pLEICS-05_*Pf*CLK3 (residues-1-669-5xHIS)) were used to transform BL21 Codon Plus (DE3) *Escherichia coli* competent cells (Agilent Technologies). Protein expressions were induced for 4 hours at 37°C for *Pf*CLK3 and at 22°C for *Pf*CLK1 after the addition of 0.1 mM isopropyl β-D-1-thiogalactopyranoside (IPTG). Cell pellets were lysed by sonication in Lysis Buffer (20 mM Tris/HCl, pH 8.0, 300 mM NaCl, 1 mM DTT and 10 mM Imidazole) and EDTA-free protease inhibitor cocktail, followed by centrifugation at 8000 g. Clarified supernatants were loaded onto Ni-NTA Superflow cartridges (Qiagen), washed using lysis buffer, and eluted with lysis buffer containing 300mM Imidazole. Protein was dialysed in buffer containing 20 mM Tris/HCl, pH 7.4, 150 mM NaCl, 1 mM $MgCl_2$ and 10% glycerol and aliquots were stored at -80°C.

Expression and purification of *Pf*CDPK1 and *Pf*PKG recombinant proteins was conducted as described previously (5).

**Kinase assay optimisation for high throughput screen**

Enzyme kinase assays were conducted in 10µL reaction volume at room temperature for 1 hour in buffer containing 50 mM HEPES pH 7.5, 10 mM $MgCl_2$, 1 mM EGTA, 2 mM DTT and 0.01% Tween20 in a black 384-well microplates (Greiner Bio-One). U*Light*™ substrates, Europium labelled anti-phospho-U*Light*™, and 10X Detection Buffer were purchased from Perkin Elmer. U*Light*-CREBtide (Sequence: CKRREILSRRPSYRK) and U*Light*-MBP peptide (sequence: CFFKNIVTPRTPPPSQGK) were the substrates of choice for *Pf*CLK1 and *Pf*CLK3, respectively. To determine $K_m$ ATP, Serial dilutions of ATP from 1000 or 500 µM were added to the reaction wells containing *Pf*CLK1 + U*Light*-CREBtide or *Pf*CLK3 + U*Light*-MBP in 384

well black microplates (Greiner Bio-One). End point 665/615 nm data were fit to the Michaelis-Menten equation using GraFit version 5.0.12 (Erithacus Software Ltd.)

Reactions were performed using ATP at $K_m$ concentration and optimized U*Light*™ and kinase concentrations (30 µM ATP with 5nM *Pf*CLK1 and 10µM ATP with 50nM *Pf*CLK3). Kinase reactions were stopped by addition of the Detection Mix Solution containing 10 mM EDTA and 1 mM anti-phospho-U*Light*™ in 1X Detection Buffer and the TR-FRET signal (emission1 = 665 nm, emission2 = 615 nm) was acquired after 1-8 hours using an EnVision™ Multilabel plate reader (Perkin Elmer, Waltham, MA).

Miniaturization to 1536-well format was possible and final assay performance was assessed by calculation of means and standard deviation of standard inhibition curves. Signal-to-background ratios S/B of 10 and 5 and Z´-values of 0.8 and 0.6 were calculated for *Pf*CLK1 and *Pf*CLK3, respectively, suitable for HTS.

**High throughput Screening**

GSK compounds from the Tres Cantos Antimalarial Set (TCAMS, 13194 compounds), and Protein Kinase Inhibitor Set displaying known anti-plasmodial activity (PKIS, 1115 compounds), and MRC-Technology index library (MRCT, 9970 compounds) were screened in single shot against *Pf*CLK1 and *Pf*CLK3. Kinase inhibitor-like compounds from the MMV Malaria Box (a selection of 260 from the original 400 compound library) were screened against *Pf*CLK1 and *Pf*CLK3 in dose response experiments (n=2), together with hits obtained from the Single Shot Screen.

Compounds were tested in single shot at 10 µM, or in dose response from 100 µM (11-point, 3-fold serial dilutions). Screening was performed in 1536-well plates, with final reaction and read-out volumes of 4 µL and 6 µL, respectively.

40 nL of 100x compound, or 40 nL DMSO (columns 11&12 - maximum and 35&36 - minimum activity controls) were dispensed onto each plate using an Echo Liquid handler. 2µL of 2x PfCLK or kinase buffer were added onto all plates except columns 35 & 36 (no enzyme, minimum activity control), where 2 µL of kinase buffer were added. Reactions were initiated upon addition of 2x Substrate Solution containing $K_m$ ATP concentration and U*Light*-MBP or U*Light*-CREBtide for *Pf*CLK3 and *Pf*CLK1, respectively. Solutions were dispensed with a Multidrop Combi (Thermo Fisher Scientific, Waltham, MA, USA) and TR-FRET readouts were collected using an EnVision™ multilabel plate reader (Perkin Elmer) and normalized to control values of uninhibited and no enzyme.

The results from the High-Throughput screening were further analysed using Activity Base (ID Business Solutions Ltd., Surrey, UK). For each test compound, % inhibition was plotted against compound concentration. To calculate $IC_{50}$, data was fit to the standard single-site four-parameter logistic equation:

$y = \{(Y_{max} – Y_{min})/[1 + ([I] / IC_{50})^n]\} + Y_{min}$

Where, $Y_{max}$ is the maximum response, $Y_{min}$ is the baseline, [I] is the concentration of compound, n is the Hill slope, $IC_{50}$ is the inflection point concentration. In cases where the highest concentration tested (i.e., 100 µM) did not result in greater than 50% inhibition, the $IC_{50}$ was determined as greater than 100 µM. $pIC_{50} = -\log IC_{50}$, expressing the $IC_{50}$ in molar units.

**Parasite culture**

*P. falciparum* cultures were maintained in RPMI-1640 media (Invitrogen) supplemented with 0.2% sodium bicarbonate, 0.5% Albumax II, 2.0 mM L-glutamine (Sigma) and 10 mg/L

gentamycin. Human blood group O, Rh +ve were used for parasite culture and cultures were maintained at 5% carbon dioxide, 5% oxygen and 90% nitrogen mixed gas incubator at 37$^{o}$C. *P. knowlesi* A1-H.1 parasites were maintained in RPMI-1640 media supplemented with 0.2% sodium bicarbonate, 10% horse serum (Gibco), 0.5% Albumax II , 2.0 mM L-glutamine, 10 mg/L gentamicin. Schizont enrichment was performed via centrifugation at 900 x g for 12 minutes by layering the parasite culture on top of a 55% (v/v) Nycodenz (Axis Shield) cushion diluted from a 27.6% Nycodenz (wt/vol) stock solution in 10 mM HEPES, pH 7.4. For drug assays, schizonts enriched from a semi-synchronous culture were added to fresh RBCs and adjusted to a 0.5% parasitaemia following reinvasion.

**Evolution of compound-resistant lines and whole genome sequencing**

The *P. falciparum* Dd2 strain was cultured in triplicate in the presence of increasing concentrations of TCMDC-135051 to generate resistant mutants as previously described(*42*). After approximately 60 days of selection parasites were cloned in 96-well plates by limiting dilution(*43*). The half maximal (50%) inhibitory concentration was determined in dose-response format using a SYBR Green-I based cell proliferation assay as previously described(*41*). To determine genetic variants that arose during selection genomic DNA was isolated from each parasite strain. 250 base pair paired-end DNA libraries were prepared using the Illumina Nextera-XT method and sequenced on an Illumina Mi-seq according to manufacturer's instructions. Reads were aligned to the *P. falciparum* 3D7 reference genome (PlasmoDB v9.0) as previously described(*45*). Single-nulceotide variants were detected using the Genome Analysis Toolkit (GATK v1.6) and the filtered based on the distribution of each quality control parameter (QD < 15.0, SQR > 1.9, MQ < 50.0, DP > 2700,

MQRankSum -11.3 < x < 11.3, Qual > 400, DP > 6, GQ > 15.0, ReadPosRankSum -12.3 < x < 12.3, snp cluster: 3 in a window of 10.

**Blood stage development inhibition assay by microscopy**

Parasite cultures were tightly synchronized by two Percoll treatments in a span of one hour followed by sorbitol treatment to remove any left over schizonts after the second Percoll treatment and the very early ring stage parasites (0-1 Hour) were collected which were used to monitor inhibition of blood stage development of the parasite following treatment with inhibitor. Synchronized parasite cultures were treated with 1 μM TCMDC-135051 at time point 0, 10, 20, 30 and 40 hours and thin smears from each treatment or no treatment were prepared at time point 0 hour, 10 hour, 20 hour, 30 hour, 40 hour, 50 hour and 70 hour. Thin smears were stained with Giemsa's stain and images of the parasites were acquired under light microscope at 100X magnification to study the stages of parasite blood stage development affected by the inhibition of *Pf*CLK3.

**Asexual $EC_{50}$ determination**

Early ring stages of *P. falciparum* cultures were plated in 96-well black plate with clear bottom at 2 % hematocrite and 0.3 % parasitaemia. Serial dilations of compound TCMDC-135051 staring at maximum 100 μM final concentrations were added to the parasite culture in triplicate and three wells were included with no drugs as control. Parasite cultures were incubated at 37°C for 72 hours and the viability of parasites in each condition were measured by staining parasite nuclei with nucleic acid stain SYBR Green (Invitrogen). Excitations at green channel were acquired on ClarioStar and the data were analyzed by Prism software.

**Parasite reduction rate assay**

Ring stages of 3D7 parasite clone were treated with TCMDC-135051 corresponding to 10X $EC_{50}$ of the inhibitor concentration at blood stage development inhibition assay ($EC_{50}$-188nM using hypoxanthine incorporation assay). Parasite cultures were treated for 120 hours with drug being renewed every 24 hour during the treatment. Samples of drug treated parasites were collected every 24-hour (24, 48, 72, 96 and 120 hour time points) and drug was washed from the collected sample by two rounds of centrifugation. Drug free parasites were diluted by three fold limiting dilution and cultured for 28 days in microtitre plates. These experiments were repeated four times (n=4). Samples were collected on 21 day and 28 day from the microtitre plate and parasite viability assessed by hypoxanthine incorporation assay. For the hypoxanthine incorporation assay, 100μl of parasite cultures were supplemented with 8 μl of 0.025mci/ml $^{3}$H-hypoxanthine and parasite cultures were maintained for 72 hours and incorporation of $^{3}$H-hypoxanthine measured by counting radioactivity in each well. Treatment with pyrimethamine was also conducted in parallel as control and previous data for artemisnin, atovaquone and chloroquine were included to allow comparative analysis of the killing profile.

**Generation of G449 mutant parasite**

Fragment of *Pf*CLK3 gene containing part of exon2, exon 3, exon 4 and part of exon 5 (1143 bp) corresponding to 655-1797 bp in clk3 genomic sequence was amplified using primer CLK3-HR1 and CLK3-HR2 and the amplified product named as *Pf*CLK3 Homologous region (CLK3-HR) was cloned in pHH1 derived vector using restriction sites HpaI and BglII. The rest of clk3 gene sequence down stream of CLK3-HR corresponding to 1798-3152 bp *Pf*clk3

genomic sequence were modified by removing introns and the stop codon and the coding sequence was optimized for *E.coli* codon usage to make it dis-similar to *Pf*clk3 genomic sequence. This fragment of gene which we named as *Pf*CLK3-codon optimized (CLK3-CO) was commercially synthesized and included BglII recognition site at 5' and XhoI recognition site at 3'. CLK3-CO was cloned downstream of CLK3-HR region in the parent plasmid using BglII and XhoI restriction sites in such a way that the triple HA tag sequence in the parent plasmid remained in frame with the *Pf*clk3 sequence. The BglII restriction site that was artificially introduced for cloning purpose was mutated back to original *Pf*CLK3 coding sequence by site directed mutagenesis using CLK3-BglII-KN1 and CLK3-BglII-KN2 primers. Site directed mutagenesis was used again to mutate Glycine in *Pf*CLK3 at position 449 to an alanine residue using CLK3-G449P1 and CLK3-G449P2 primers. The target vector generated was sequenced to confirm the desired sequence of *Pf*clk3 in the plasmid and further confirmed that 3-HA sequence is in frame with clk3 coding sequence. 10 μg of the target vector was used for transfection of schizont stage of the parasite using Lonza nucleofactor following the protocol as has been published by (45). Transfected parasites were cultured under selection drug pressure (2.5nM WR99210) till ring stage of the parasites could be seen in Giemsa stained smear. The parasites were maintained under drug OFF (three weeks) and drug ON (three weeks) pressure for two cycles to eliminate the parasite where the target plasmid was maintained episomally. Following drug cycle clones of parasite were generated by limiting dilution and the integration of target plasmid at the *Pf*clk3 genomic locus of the cloned parasite was confirmed by PCR amplification of 1493 bp gene fragment using primers P3 (448-478 bp in *Pf*clk3 genomic locus, upstream of *Pf*CLK3-HR region) and P4 (1923-1940 bp sequence in clk3 gene of transgenic parasite, part of CLK3-CO region in target plasmid) which could be generated only if the target plasmid is integrated at the clk3

genomic locus. At the same time PCR amplification using primers P1 (571-605 bp in clk3 genomic locus, upstream of CLK3-HR region) and P2 (1825-1852 bp in *Pf*clk3 genomic locus, in a region which is replaced by CLK3-CO region in transgenic parasite) did not show amplification in CLK3-G449P clones (A3 and A8), which confirms that the wild type *Pf*clk3 locus was destroyed in the transgenic parasites. Amplification of 1282 bp product using primer P1 and P2 confirms that these primers can amplify clk3 at genomic locus of wild type 3D7 parasites.

**Western blotting**

Parasite lysate from 3D7 wild type parasite and two CLK3-G449P clones (A3 and A8) using lysis buffer containing 20 mM Tris pH-8.0, 150 mM sodium chloride (NaCl), 1 mM di-thiotritol, 1 mM ethylenediaminetetraacetic acid (EDTA), 1% IGEPAL CA630 detergent and protease and phosphatase inhibitor mix. Parasite lysates were cleared by centrifugation at 21000xg for 5 minutes and 20 μg of parasite lysate were separated on 8% polyacrylamide gel under reducing condition. Proteins were transferred to nitrocellulose membrane and the membranes were blocked for two hour with blocking buffer that contain 20 mM Tris pH 7.4, 150mM NaCl, 0.1% Tween-20 and 5% skimmed milk. Following blocking the membranes were incubated with primary antibodies (Anti-HA monoclonal antibody or anti-*Pf*CDPK1 polyclonal antibody) at 1:1000 dilution in blocking buffer for one hour. The membranes were washed four times, each of 15 minutes, with wash buffer (blocking buffer without milk) and incubated with goat anti-rat HRP conjugated antibody at 1:2000 dilution in blocking buffer for one hour. Following this incubation the blots were washed four times with wash buffer and developed using enhanced chemi-luminiscence kit. The luminescences

from the blots were acquired on X-ray film. The control gel following electrophoresis was stained with Coomassie stain to show equal loading.

**DNA Microarray experiment**

Microarray was used to study changes in transcript level in the parasite following treatment with CLK3 inhibitor. Trophozoite stage of wild type (Dd2) or mutant (051C) parasites were purified using MACS (magnetic assisted cell sorting, Milteny Biotec) purification column and treated either with compound TCMDC135051 (1μM) or solvent DMSO for one hour at 37°C. Following inhibitor treatment the parasites were treated with 0.1% saponin in phosphate buffer saline (PBS) for one minute on ice to release parasites from host erythrocyte. Parasites were washed twice with PBS and the parasite pellets were used for total RNA isolation using RNeasy Lipid Tissue Kit (Qiagen). Bioanalyzer 2100 instrument (Agilent) was used to assess the integrity of RNA samples and samples with RNA integrity score of >8 were used for the array experiment. cDNA was prepared from the RNA samples using cDNA synthesis kit (Agilent) and equal amounts of cDNAs (amount 200ng) were labeled with Cy3 label and the equal incorporation of label was confirmed by NanoDrop. Custom DNA microarray slides were prepared (Agilent) that contained 14353 unique probes covering 5752 *P. falciparum* genes as described before by(*31*). Microarray slides were hybridized with labeled cDNA samples and intensity of label in each probe of the array were acquired by Agilent G2505C Microarray scanner. Normalized data from four independent biological replicates were used to identify probes showing at least two-fold change between the control samples and inhibitor treated samples. Statical significance (p-value 0.5<) between the control and treated samples were calculated using moderate T-test analysis.

**Liver stage development assay**

*Plasmodium berghei* sporozoites expressing Luciferase were freshly collected from salivary gland of *Anopheles stephensi* mosquitos to be used for measurement of inhibition of exoerythrocytic form (EEF) development by drug treatment. The freshly collected sporozoites were used for infection of human hepatocarcinoma HepG2 cells expressing the tetraspanin CD81 receptor (HepG2-A16-CD81EGFP cells). HepG2 cells were pretreated for 18 hours with the inhibitor before infection with *P. berghei* sporozoites. After infection, the HepG2 cells were further treated with the drug at concentrations shown for 48 hours and the inhibition of EEF development were measured by bioluminescence. Atovaquone and DMSO treatments were used as positive and negative controls in the microtitre based plate assay. $pEC_{50}$ value of the inhibitor for inhibition of sporozoite development were generated using bioluminescence values.

***P. berghei* blood stage development assay**

*P. berghei* ANKA strain of parasite was used for infection of Balb/c mice. Blood of *P. beghei* infected mice were collected at parasitaemia of 1-3% and the parasites were allowed to grow in *in vitro* for 24 hour, which allowed the parasites to synchronize at late schizont stage. Mice were infected with late schizont *P. berghei* parasites for 2-4 hours that allowed schizonts to rupture and form nascent ring stage of the parasite. Ring stage parasite infected RBCs were collected from the mice and treated with drug at eight-point dilution for 22-24 hours at $37^0$C in a microtitre plate. Following inhibitor treatment, parasites were stained with Hoechst DNA stain and acquired by flow cytometry to measure percentage of schizont-infected cells. Artemisinin and DMSO treatments were used as positive and negative control. Growth inhibitory concentrations were calculated using Prism 7 software.

**Stage II gametocyte inhibition assay**

*P. falciparum* Pf2004 strain of parasites expressing tdTom as marker for stage II gametocyte were used to measure inhibition of gametocyte development by the inhibitor, as previously described (46). At 28 hours post invasion (28hpi) the regular culture medium was replaced with serum-free medium (-SerM) complemented with a minimal fatty acid mixture and bovine serum albumin (0.39% fatty acid-free BSA and oleic and palmitic acid [30 μM each; added from 30 mM ethanol-solved stocks]) to induce sexual commitment. After 20 hours of incubation in -SerM the medium was replaced with complete medium containing 10% serum for the remainder of the experiment. Inhibitor at eight-point dilutions starting at 20μM was added at 28hpi, and it was maintained for 42 hours to study the effect of the inhibitor on early gametocyte (stage II) development. Following treatment gametocytaemia was measured by flow cytometry using tdTom reporter fluorescence as a viability marker (details on cytometry are given in (46). The inhibitory effect of the compound on gametocyte development was calculated using Graph Prism 7 software.

**Gametocyte culture and exposure to drug**

Gametocytes of *P. falciparum* clone 3D7 were generated *in vitro* using standard methodology to produce infectious gametocytes (47), using human blood obtained from the Scottish National Blood Transfusion Service and medium containing heat-inactivated human serum at 10% (v/v). Gametocyte flasks were prepared to enable a mixture of D14 and D17 cultures to be fed to mosquitoes on the day of the infectious feed. Medium was changed daily for all cultures.

The gametocytes were exposed to drug in two ways. For longer exposure times, the cultures were split into 6 separate flasks once they had reached stage II, and from that stage on the medium used was supplemented with drug at concentrations of 0.25, 0.5, 1, 2 and 4 µM, with medium for the control flask being supplemented with an equivalent amount of the drug solvent DMSO. For shorter exposure, separate stage V gametocyte flasks were split 24 hours before the feed, and exposed to medium containing 1 or 2 µM of drug.

**Infection of mosquitoes**

*Anopheles coluzzii* (Ngousso strain) mosquitoes were reared under standard insectary conditions (26±1°C, 80% humidity, 12 hr light:12 hr dark cycle). Adult mosquitoes were fed *ad libitum* on 5% glucose solution containing 0.05% (w/v) 4-aminobenzoic acid (PABA). Five to seven day old female mosquitoes were infected by membrane feeding of gametocytes using standard procedures (47). Briefly, gametocytes were pelleted from the cultures by centrifugation, resuspended in equal volumes of serum, containing the same concentration of drug they were previously exposed to), and mixed with 1-2 volumes of uninfected fresh blood at 40% haematocrit made up in serum containing the same concentration of drug. The final gametocytaemia in the infectious blood meal was always above 0.7%, but varied between experiments.

Mosquitoes were allowed to feed for 10 minutes. Exflagellation was monitored during this period by microscopical observation (400x magnification) of a drop of the feed material under a coverslip. Exflagellating centres were counted over 50-100 fields. Unfed mosquitoes were removed from the pots. Mosquitoes were maintained under insectary conditions and fed *ad libitum* on 5% glucose solution containing 0.05% (w/v) 4-aminobenzoic acid (PABA).

Mosquitoes were examined for oocyst infections 10-11 days after the feed by removal of the midgut and examination of the entire gut for oocysts at 400x magnification.

and medium containing heat-inactivated human serum at 10% (v/v). Prevalence of oocysts in mosquitoes was calculated as the number of mosquitoes with oocyst infection / number of mosquitoes dissected.

To test for the effect of TCMDC-135051 on gametocyte development and mosquito infection, data were analysed with a generalized linear mixed-effect model (GLMM) using the package lme4 (version 1.1-19) (48) in R (version 3.4.2) (49). Count data, such as gametocyte numbers and exflagellation were analysed using GLMMs with poisson error, and prevalence of infection was analysed using GLMMs with binomial errors. All GLMMs included experiment number as a random effect. The residuals of the models (diagnostics) were assessed using visual inspection of residual versus predicted values (Homogeneity of variance), Shapiro-Wilk tests (normality), and the R package aods3 (overdispersion). In all cases the optimal model was selected by backward elimination of the maximal model containing all fixed effects and their interactions of interest, and the random effects (50). The variance in the predictor variable explained by the GLMM (both marginal and conditional R squared values, delta method) were calculated using the package MuMIn (v1.42.5), implementing the methodology of Nakagawa, Johnson and Schielzeth (51).

### *In vivo P. berghei* infection and drug treatment

Drug efficacy in *P. berghei* was assessed using standard Peters four day suppression test. Briefly, *P. berghei* ANKA strain line 820cl1m1 parasites ($1x10^5$) were intraperitoneally (i.p.) injected into mice at day zero. Drug dosing started 1.5 hours after injecting parasites. Stock TCMDC-135051 was prepared in 1:1 mixture of DMSO and Tween-80 and diluted 10 fold in

sterile distilled water for a final vehicle concentration of 5% Tween-80 and 5% DMSO. Control mice were dosed with vehicle (5% Tween-80 5% DMSO) twice daily or chloroquine (20mg/kg in 1XPBS). All drug and vehicle injections were delivered by i.p. Parasiteamia was monitored daily from day 4 by taking blood smears and flow cytometry. Percentage parasite suppression was calculated on Day 4 using the formula: 100 – (mean parasitaemia in treatment group/mean parasitaemia in vehicle * 100).

**Expression and purification of human PRPF4B**

The kinase domain (residues 669-1005) of human PRPF4B was cloned into vector pFB-LIC-Bse (GenBank ID EF199842) downstream of an amino-terminal tag of 23 residues consisting of a hexa-histidine tag (6xHis) and a TEV-protease site for tag removal. The resulting plasmid was used to generate bacmid DNA in *E. coli* DH10Bac cells, followed by virus assembly in Sf9 cells (Invitrogen Bac-to-Bac Expression System). For the expression of PRPF4B, 2 L cultures of suspended Sf9 cells were grown at 27°C in Insect-XPRESS media (Lonza) to a density of 2 x $10^6$ cells/mL, before being infected with P2 baculovirus. After 72 h, cells were harvested by centrifugation at 900 × g for 30 minutes at 4$^{o}$C. The cell pellet was resuspended in Lysis Buffer (50 mM HEPES pH 7.5, 500 mM KOAc, 50 mM arginine, 50 mM glutamate, 10 mM imidazole, 10% glycerol, 2 mM TCEP and protease inhibitor cocktail (Millipore Set III)) and stored at -85$^{o}$C until use. To purify PRPF4B protein, cells were disrupted by sonication in 5 cycles of 5 second pulses (35% max amplitude, Sonics VCX750) with 10 second intervals, on ice. To clear up debris, polyethyleneimine pH 7.5 was added to the lysate to a final concentration of 0.15% (w/v) and the sample was centrifuged at 20,000 × g for 45 min at 4°C. The supernatant was loaded onto a 5 mL HisTrap FF Crude column (GE Healthcare) which was washed in Lysis Buffer containing 30 mM imidazole until the UV absorbance

reached baseline, before PRPF4B elution by isocratic wash in 10 column-volumes of Lysis Buffer containing 300 mM imidazole. In order to cleave the N-terminal 6xHis-tag, PRPF4B was mixed with N-terminal His-tagged TEV protease (about 15:1 molar ratio of kinase to protease) and dialyzed overnight at 4$^{o}$C against 20 mM HEPES pH 7.5, 500 mM KOAc, 50 mM arginine, 50 mM glutamate, 5% (v/v) glycerol, 2 mM TCEP. PRPF4B was then re-purified by affinity chromatography on Ni-sepharose followed by gel filtration on a Superdex 200 16/60 column (GE Healthcare) pre-equilibrated in 20 mM Tris·HCl pH 8.0, 200 mM NaCl, 5 mM TCEP. The elution peak was analyzed by SDS-PAGE, pooled and concentrated to 16 mg/mL by ultrafiltration (Centriprep devices with 10 kDa MW cut-off). The final sample concentration was determined by UV absorbance using a NanoDrop spectrophotometer (Thermo Scientific) with the calculated molecular weight of 39.54 kDa and estimated extinction coefficient of 27,850 $M^{-1}.cm^{-1}$ at 280 nm.

**Differential scanning fluorimetry (DSF) analysis.**

PRPF4B protein was thawed from storage, diluted to 2 µM in ice-cold buffer containing 50 mM HEPES pH 7.5, 150 mM NaCl, 10 mM $MgCl_2$, 1 mM EGTA and 5X SYPRO orange dye (Invitrogen, S-6650). Protein/dye solution was transferred to a 384-well PCR plate with 25 µL/well plus 0.5 uL of 1 mM test compounds in DMSO (2% final DMSO concentration). Thermal shift data was acquired in a qPCR instrument (Applied Biosystems QuantStudio 6) programmed to equilibrate the plate at 25$^{o}$C for 5 min followed by ramping the temperature from 20 to 95$^{o}$C at a constant rate of 0.05$^{o}$C per sec. Data was processed using Protein Thermal shift software (Applied Biosystems) fitting experimental curves to a Boltzmann function to calculate differential thermal shifts (dTm) referenced to protein/dye in 2% DMSO.

**PRPF4B enzymatic assay.**

Enzyme activity was measured using 100 nM human PRPF4B in an assay buffer consisting of 20 mM HEPES pH 7.5, 250 mM NaCl, 10 mM $MgCl_2$, 2.5% glycerol and 1 mM DTT plus 10 µM of a modified PAK4 peptide ([biotin]-GGGRDSPPPPAR-[OH]) and 2 mM ATP in a total volume of 100 µL, incubated at 30$^{o}$C for 4 h. The final assay pH was measured as pH 7.5. To stop the reactions and prepare samples for mass spectrometry analysis, 40 µL of reaction volume was taken and 20 µL of 3% formic acid was added. For measuring the effect of TCMDC-135051 on the activity of PRPF4B, we preincubated TCMDC-135051 or Compound-A (*1*) or trifluoroacetic acid (TFA) in the range of 0.005 to 100 µM (2x final concentration) with PRPF4B in assay buffer (also at 2x final concentration) for 30 min at room temperature before initiating the reaction by mixing with a 2x solution of peptide and ATP. Compound serial dilutions (3-fold) were made in 100% DMSO at 50x assay concentration before the dilution to 2x final concentration in 2x PRPF4B plus assay buffer (4% DMSO) and the final dilution to 1x concentration (2% DMSO). Compound-A, with a reported $IC_{50}$ of 16 nM against PRPF4B, was used as a control while trifluoroacetic acid, present as a counter ion in the TCMDC-135051 sample, was tested to rule out any inhibition of PRPF4B.

**Mass spectrometry (MS) analysis of PRPF4B enzymatic assay.**

The ratio between non-phosphorylated and phosphorylated PAK4 peptide was analysed by intact peptide mass analysis using 1 µL of the reaction medium by reverse phase HPLC-ESI-MS in an Acquity H-Class HPLC system (Waters Corp. Milford, MA, USA) directly connected to a XEVO G2-Xs QToF (Waters). The HPLC was equipped with a C18 column (ACQUITY UPLC Protein BEH C18 Column, 1.7 µm, 2.1 mm X 50 mm, Waters) for small molecule separation kept at 45°C. The mobile phase solvent A was 0.1% formic acid (FA) in water, and solvent B

was 0.1% FA in 100% Acetonitrile (ACN). The samples were loaded at a flow rate of 0.5 uL/min, and eluted from the C18 column at a flow rate of 400 uL/min with a linear gradient step of 3% to 90% solvent B over 2.5 min. The column was regenerated by washing at 100% solvent B for 1.5 min and re-equilibrated at 1% solvent B for 3 min. Exact mass analysis was performed in positive ion electrospray mode. For internal calibration, the LockSpray ion source properties were the following: Scan time was fixed at 0.5 sec, with a mass window of 0.5 Da around Leu-enkephalin (556.2771 Da). The ToF-MS acquisition ranged from 50 Da to 2000 Da with a scan time fixed at 0.5 sec. The cone voltage on the ESI source was fixed at 40 V. The system was controlled with MassLynx software (ver. 4.1) and data was processed using TargetLynx tool.

TargetLynx software was used to integrate the peak area of the eluted peptide from the total ion chromatogram (TIC). We focused on the following mass over charge ratios (m/z): 1389.66 (+1 charge), 695.33 (+2 charges) and 463.89 (+3 charges) for non-phosphorylated PAK4 peptide and, 1469.66 (+1 charge), 735.32 (+2 charges) and 490.55 (+3 charges) for phosphorylated PAK4 peptide. The predicted retention times were 2.7 and 2.8 min for the non-phosphorylated and phosphorylated peptide respectively. The retention times were 3.03 and 3.05 min for non-phosphorylated and phosphorylated peptides, respectively.

**Gene ontology (GO) enrichment analysis**

Gene ontology (GO) enrichment analysis was carried out using the Fisher's Exact test to compare the proportion of genes in a set annotated with each GO term with the proportion of genes in the background annotated with the same term as implemented in PlasmoDB (cite this paper: https://www.ncbi.nlm.nih.gov/pubmed/27903906). Multiple test correction was carried out using the Benjamini Hochberg method.

**DNA primers used**

**CLK1-FamB1**

AGGAGATATACATATGGATGATGAAATTGTCCATTTTAGTTGG

**CLK1-FamB2**

GAAGTACAGGTTCTCTTCAAGGAACTTGTGCTTTAATAATTCG

**CLK3-HR1**

ATGC**GTTAAC**GAAATACCATCTAATCCATCATATATCGACC

**CLK3-HR2**

ATGC**AGATCT**ATATTTTATACTACTTAATAAACGAATGATGTGCCT

**CLK3_BglII-KN1**

Cattcgaacactaagcataaatgatttttatattttatactacttaataaacgaatgatgtgccttttattgtcc

**CLK3_BglII-KN2**

Ggacaataaaaggcacatcattcgtttattaagtagtataaaatataaaaatcatttatgcttagtgttcgaatg

**CLK3-G449P1**

Gggcaatacgcagattgggccacatccattcgaaca

**CLK3-G449P2**

Tgttcgaatggatgtggcccaatctgcgtattgccc

**P1**

*GTATTTTCAGGGCGCC*Cagaatgatcagataaataaagattataacaatga

**P2**

GTGCTATTCTTAAGTTACCCCACATCCA

**P3**

CGAACACAAGAAAATGAGGATAAACTTCTAG

**P4**

CGCATGTGACGCAGGGCA

## Supplementary Figures and Tables

## Fig. S1

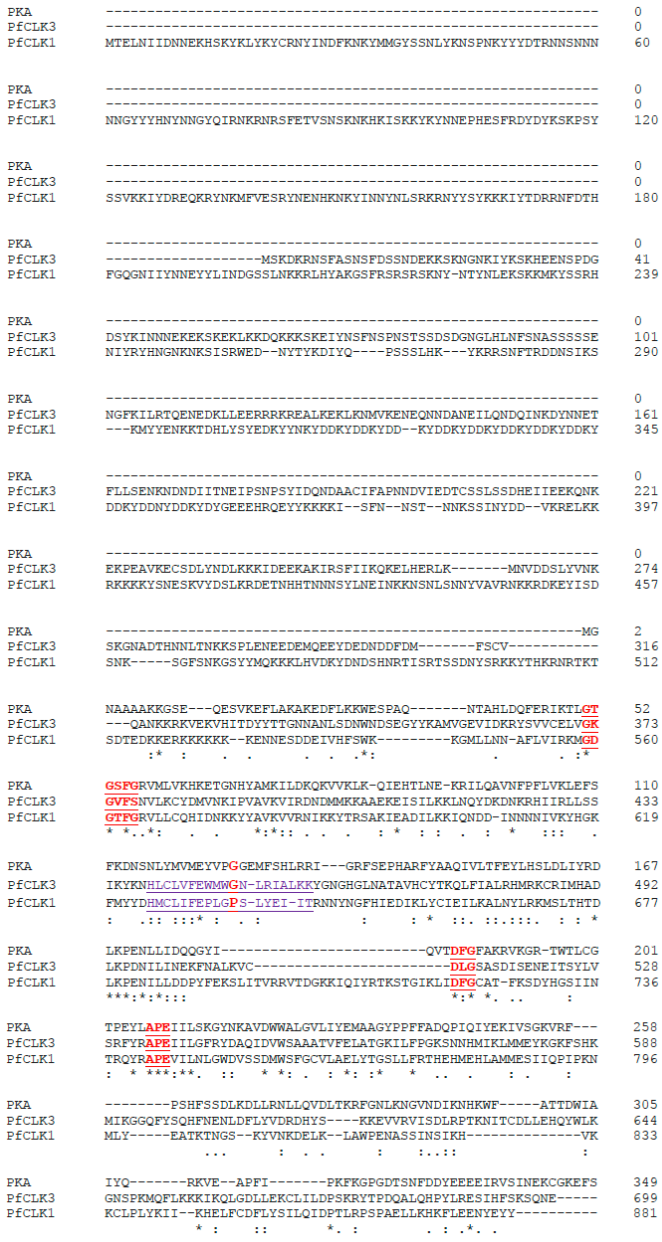

# Fig. S2

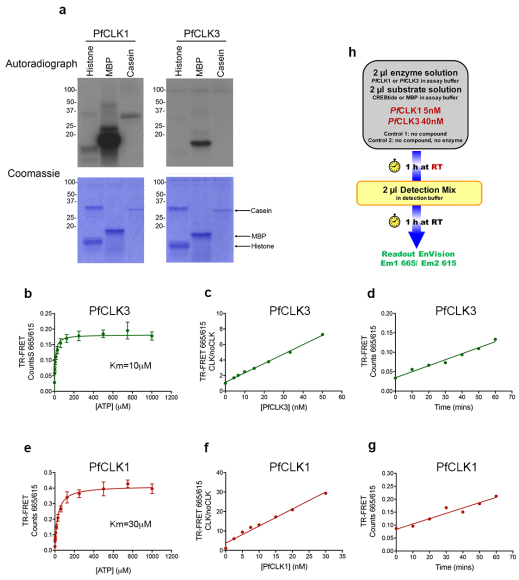
a
PfCLK1
PfCLK3
Histone
MBP
Casein
Autoradiograph
Coomassie
Casein
MBP
Histone
h
2 µl enzyme solution
PfCLK1 or PfCLK3 in assay buffer
2 µl substrate solution
CREBtide or MBP in assay buffer
PfCLK1 5nM
PfCLK3 40nM
Control 1: no compound
Control 2: no compound, no enzyme
1 h at RT
2 µl Detection Mix
in detection buffer
1 h at RT
Readout EnVision
Em1 665/ Em2 615
b
PfCLK3
Km=10µM
[ATP] (µM)
c
PfCLK3
[PfCLK3] (nM)
d
PfCLK3
Time (mins)
e
PfCLK1
Km=30µM
[ATP] (µM)
f
PfCLK1
[PfCLK1] (nM)
g
PfCLK1
Time (mins)

**Fig. S3**

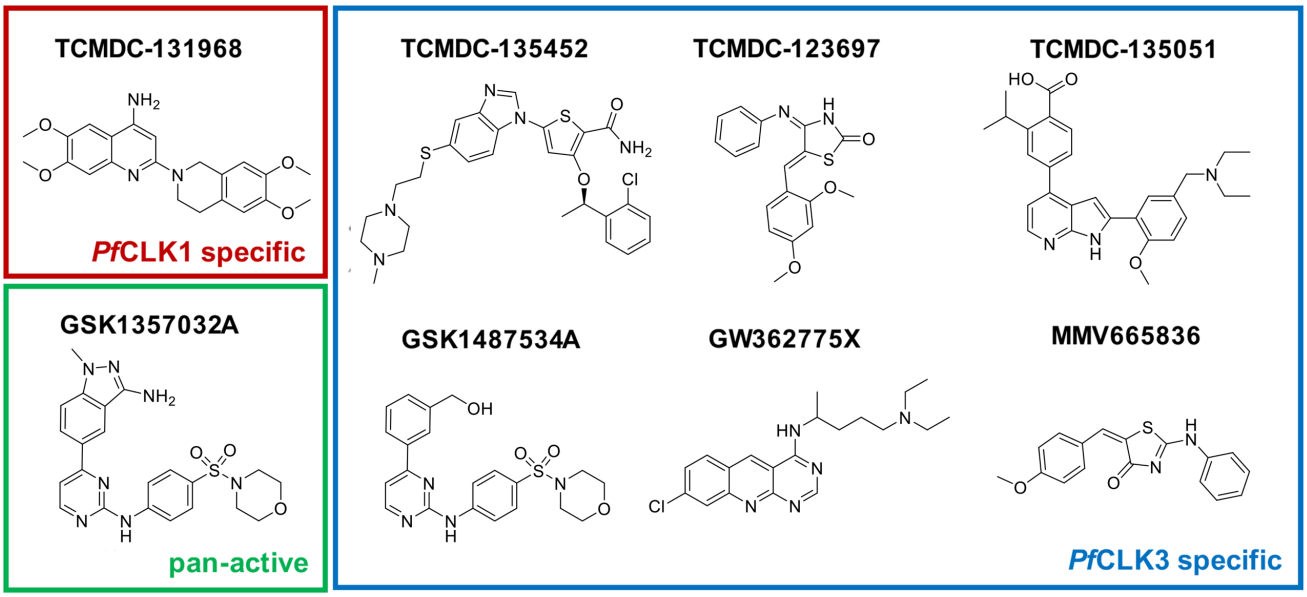
TCMDC-131968
PfCLK1 specific
GSK1357032A
pan-active
TCMDC-135452
TCMDC-123697
TCMDC-135051
GSK1487534A
GW362775X
MMV665836
PfCLK3 specific

**Fig. S4**

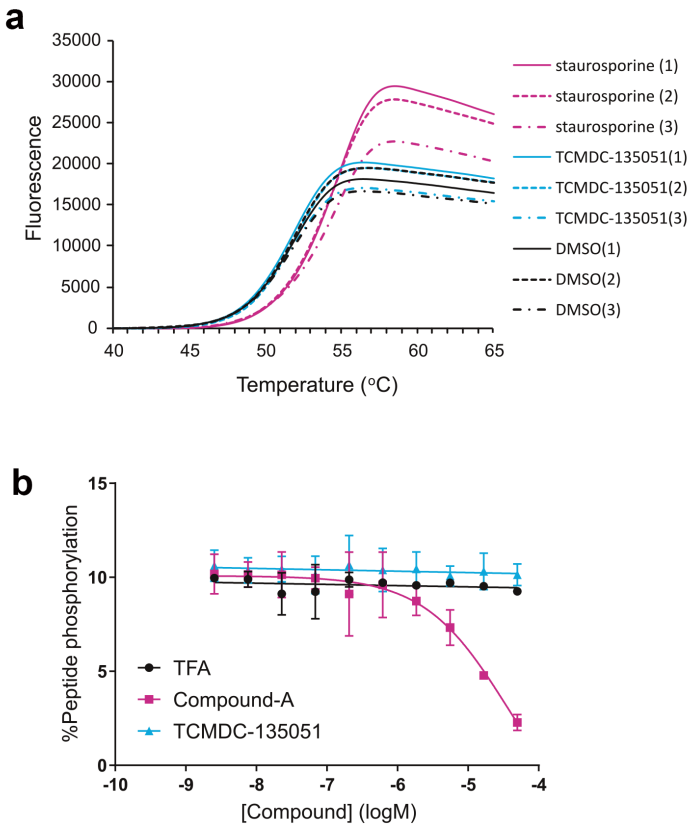
a
35000
30000
25000
20000
15000
10000
5000
0
Fluorescence
40
45
50
55
60
65
Temperature (°C)
staurosporine (1)
staurosporine (2)
staurosporine (3)
TCMDC-135051(1)
TCMDC-135051(2)
TCMDC-135051(3)
DMSO(1)
DMSO(2)
DMSO(3)
b
15
10
5
0
%Peptide phosphorylation
-10
-9
-8
-7
-6
-5
-4
[Compound] (logM)
TFA
Compound-A
TCMDC-135051

**Fig. S5**

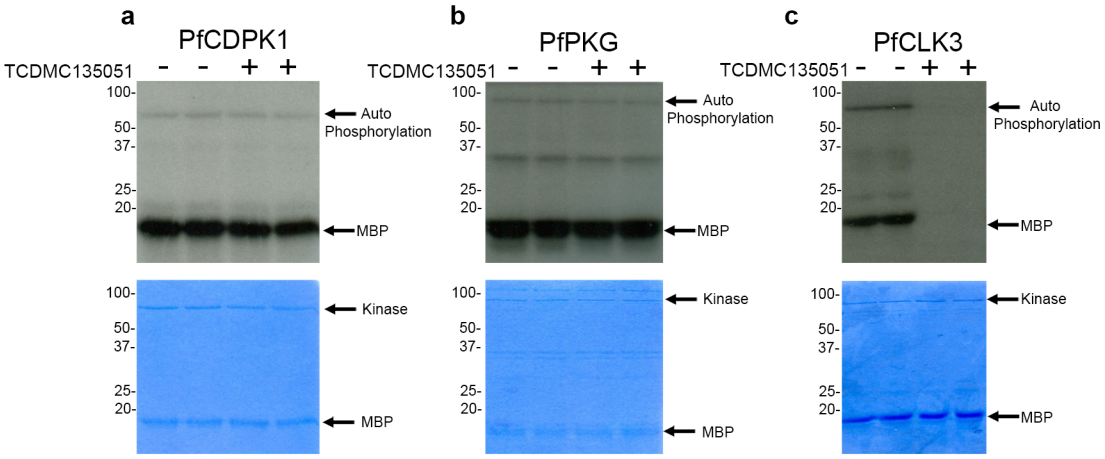
a
PfCDPK1
TCDMC135051 - - + +
100-
50-
37-
25-
20-
Auto Phosphorylation
MBP
Kinase
b
PfPKG
c
PfCLK3

**Fig. S6**

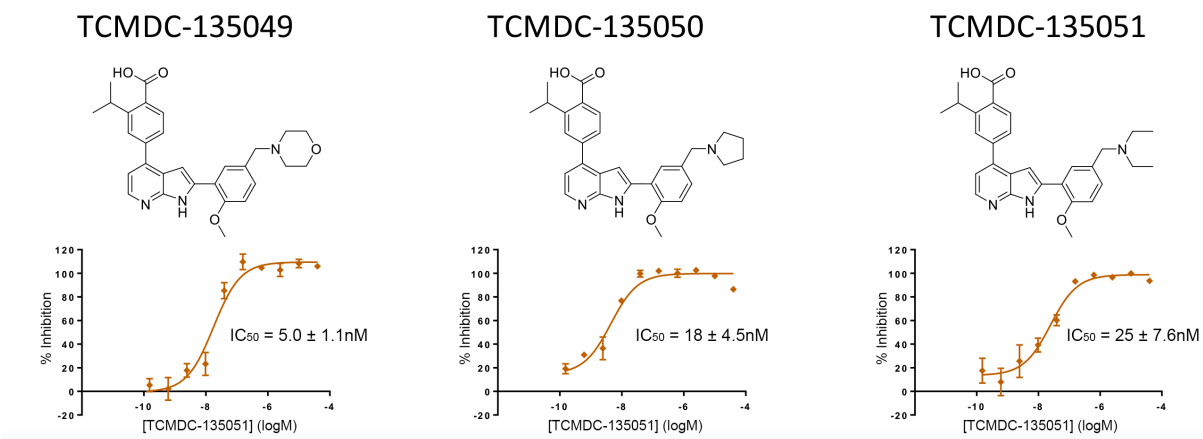
TCMDC-135049
TCMDC-135050
TCMDC-135051
HO
O
N
O
N
H
O
% Inhibition
120
100
80
60
40
20
0
-20
-10
-8
-6
-4
[TCMDC-135051] (logM)
IC50 = 5.0 ± 1.1nM
IC50 = 18 ± 4.5nM
IC50 = 25 ± 7.6nM

**Fig. S7**

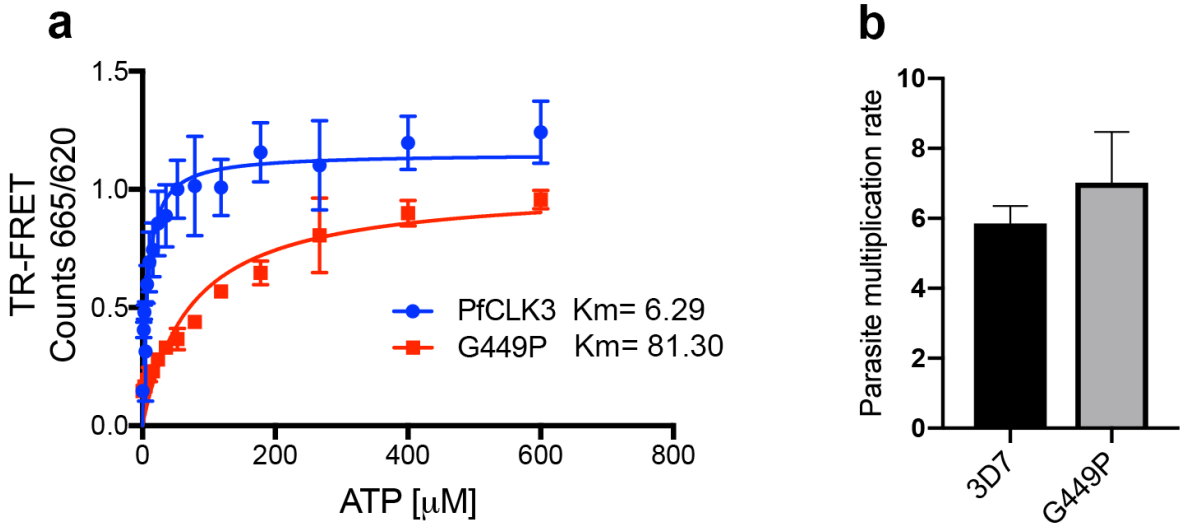
a
TR-FRET
Counts 665/620
1.5
1.0
0.5
0.0
0
200
400
600
800
ATP [μM]
PfCLK3 Km= 6.29
G449P Km= 81.30
b
Parasite multiplication rate
10
8
6
4
2
0
3D7
G449P

Fig. S8

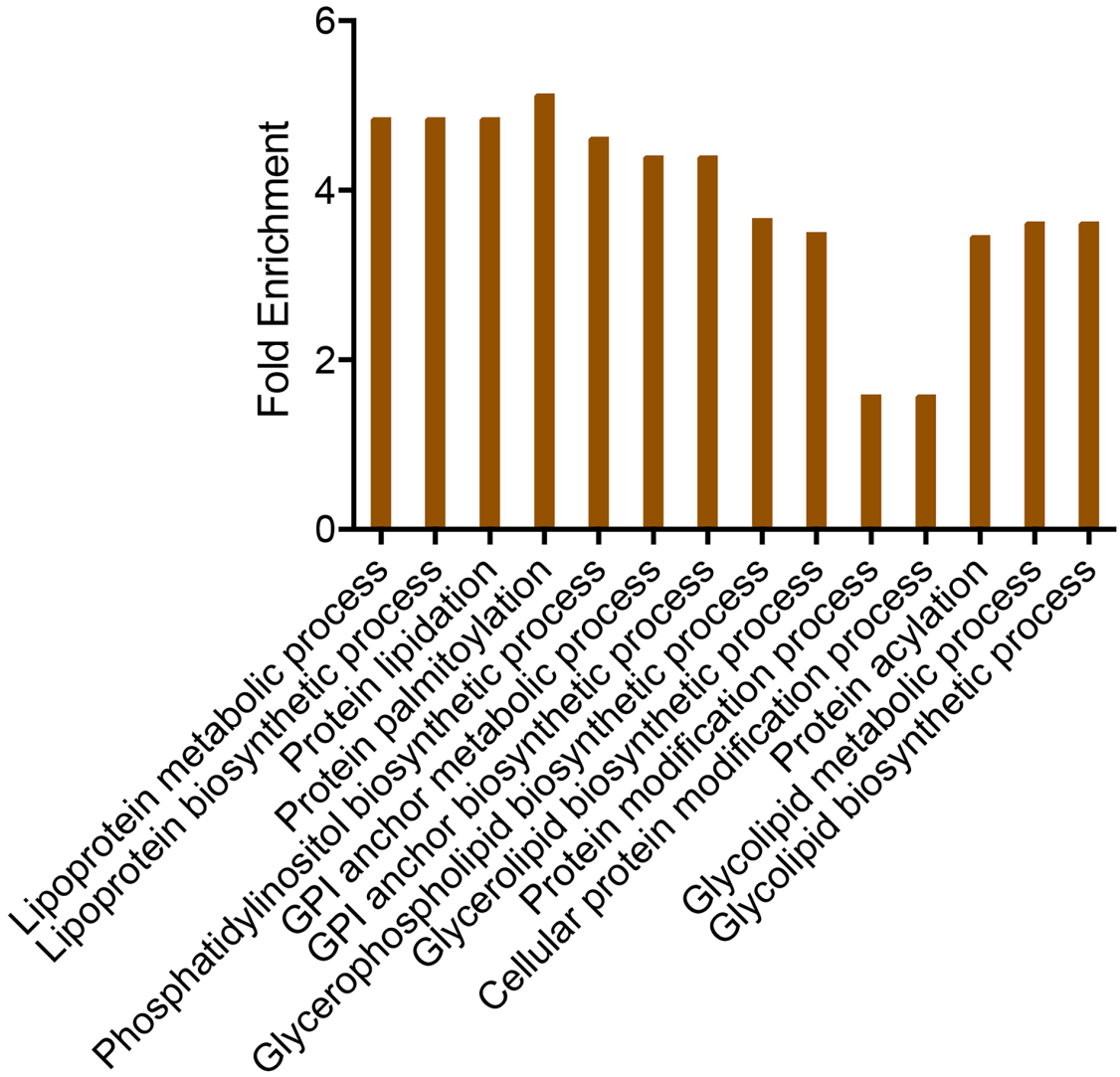
Fold Enrichment
6
4
2
0
Lipoprotein metabolic process
Lipoprotein biosynthetic process
Protein lipidation
Protein palmitoylation
Phosphatidylinositol biosynthetic process
GPI anchor metabolic process
GPI anchor biosynthetic process
Glycerophospholipid biosynthetic process
Glycerolipid biosynthetic process
Protein modification process
Cellular protein modification process
Protein acylation
Glycolipid metabolic process
Glycolipid biosynthetic process

**Fig. S9**

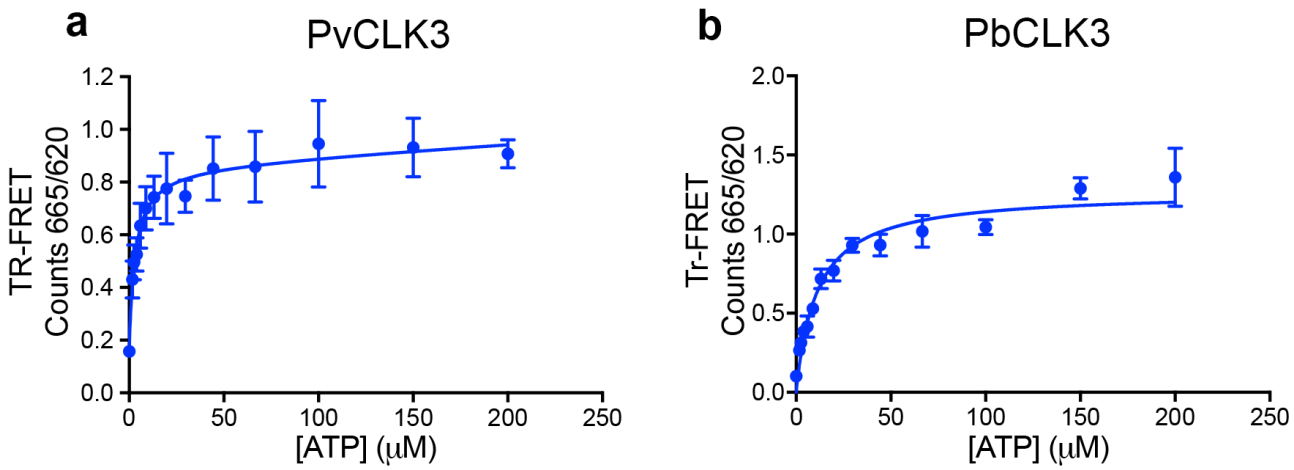
a
PvCLK3
TR-FRET
Counts 665/620
1.2
1.0
0.8
0.6
0.4
0.2
0.0
0
50
100
150
200
250
[ATP] (μM)
b
PbCLK3
Tr-FRET
Counts 665/620
2.0
1.5
1.0
0.5
0.0
0
50
100
150
200
250
[ATP] (μM)

**Fig. S10**

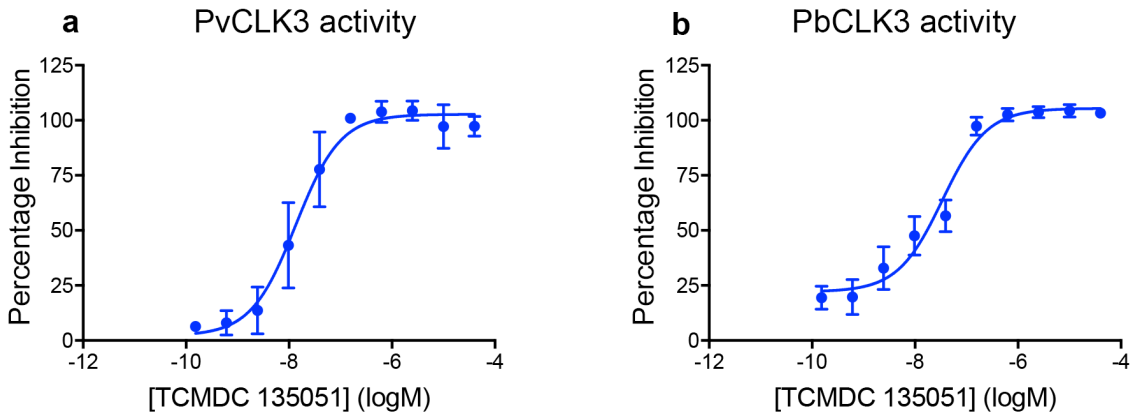
a
PvCLK3 activity
Percentage Inhibition
125
100
75
50
25
0
-12
-10
-8
-6
-4
[TCMDC 135051] (logM)
b
PbCLK3 activity
Percentage Inhibition
125
100
75
50
25
0
-12
-10
-8
-6
-4
[TCMDC 135051] (logM)

**Fig. S11**

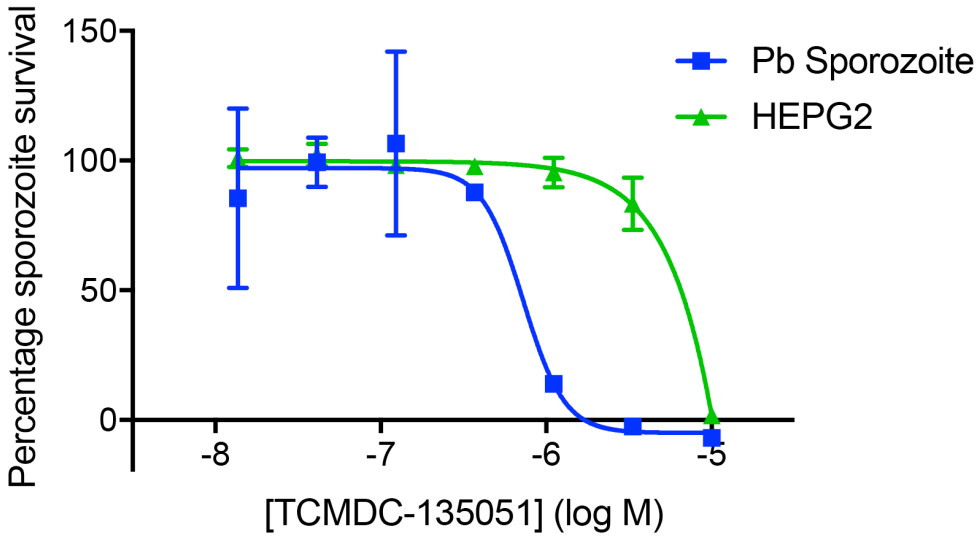
Percentage sporozoite survival
150
100
50
0
-8
-7
-6
-5
[TCMDC-135051] (log M)
Pb Sporozoite
HEPG2

**Fig. S12**

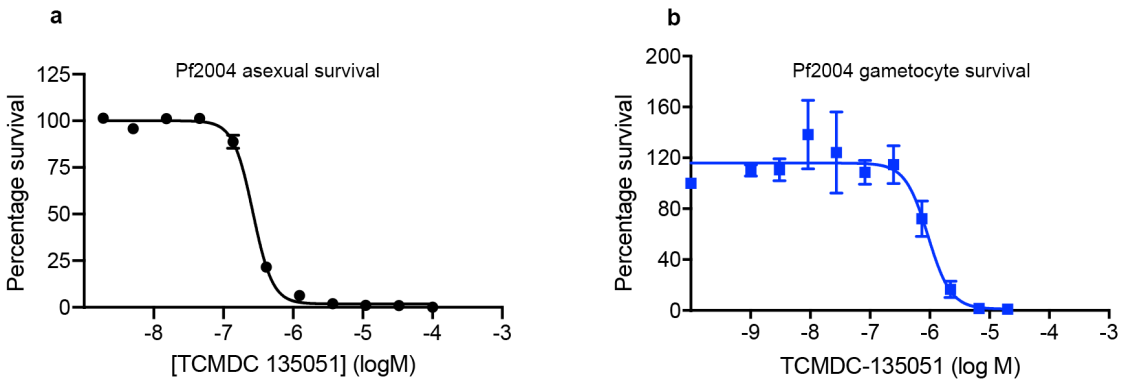
a
Pf2004 asexual survival
Percentage survival
125
100
75
50
25
0
-8
-7
-6
-5
-4
-3
[TCMDC 135051] (logM)
b
Pf2004 gametocyte survival
Percentage survival
200
160
120
80
40
0
-9
-8
-7
-6
-5
-4
-3
TCMDC-135051 (log M)

**Fig. S13**

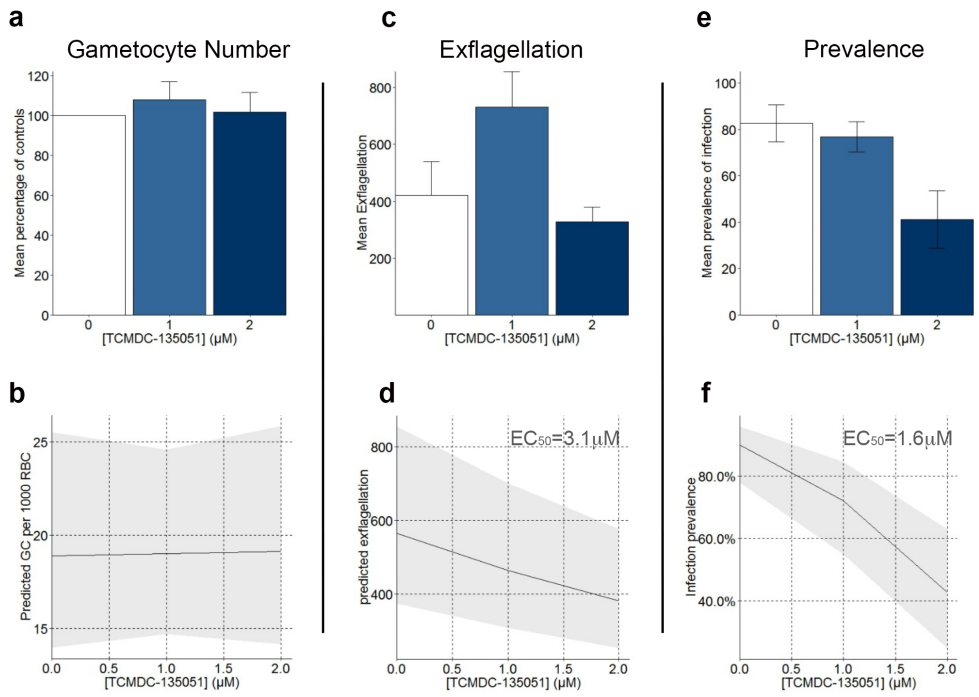
a
Gametocyte Number
Mean percentage of controls
[TCMDC-135051] (μM)
c
Exflagellation
Mean Exflagellation
[TCMDC-135051] (μM)
e
Prevalence
Mean prevalence of infection
[TCMDC-135051] (μM)
b
Predicted GC per 1000 RBC
[TCMDC-135051] (μM)
d
EC50=3.1μM
predicted exflagellation
[TCMDC-135051] (μM)
f
EC50=1.6μM
Infection prevalence
[TCMDC-135051] (μM)

**Fig. S1. Sequence alignment of *Pf*CLK1, *Pf*CLK3 and mammalian PKA**

Shown in red is the glycine rich loop, purple the kinase region V in *Pf*CLK1 and *Pf*CLK3, the glycine in position 449 in *Pf*CLK3 (which is mutated to proline in the G449P mutant described here) and corresponding amino acids in PfCLK1 and PKA (highlighted in red). Also shown are the "DFG and "APE" motifs that represent the start and finish of the activation loop, respectively. . = similar residue, : = conserved residues and the * = identical residues.

**Fig. S2. Generation of a HTS screen for *Pf*CLK1 and *Pf*CLK3**

**(A)** Gel based assay of the phosphorylation of myelin basic protein (MBP) $\alpha$-casein and histone by recombinant *Pf*CLK1 and *Pf*CLK3. The top gel is an autoradiograph and the bottom a Commassie stain of the same gel as a loading control. The position of MBP, $\alpha$-casein and histone are shown. **(B)** Measure of Vmax and Km for ATP of recombinant *Pf*CLK3 **(C)** Linear relationship between the activity read out of the TR-FRET kinase assay and the concentration of *Pf*CLK3 using in the kinase reaction. **(D)** Time course of the TR-FRET kinase reaction for *Pf*CLK1 when used at an enzyme concentration of 40nM. **(E)** Measure of Vmax and Km for ATP of recombinant *Pf*CLK1 **(F)** Linear relationship between the activity read out of the TR-FRET kinase assay and the concentration of *Pf*CLK1 using in the kinase reaction. **(G)** Time course of the TR-FRET kinase reaction for *Pf*CLK1 when used at an enzyme concentration of 40nM. **(h)** Scheme of the assay protocol for *Pf*CLK1 and *Pf*CLK3 high-throughput screens. The data shown in the graphs are the mean ±S.E.M of at least three independent experiments.

**Fig. S3. Structures of hits from the HTS screen against *Pf*CLK1 and *Pf*CLK3.**

Concentration-response curves of compounds that inhibited PfCLK1 or PfCLK3 were obtain and those compounds that had pIC50 values that were >1.5 fold different between *Pf*CLK1 and *Pf*CLK3 were considered specific whilst those that showed <1.5 fold difference in pIC values were considered as pan-active. Shown are exemplar molecules from each classification.

**Fig. S4. TCMDC-135051 does not inhibit the human orthologue of PfCLK3, PRPF4B.**

**(A)** Measurement of melting temperature of PRPF4B in the presence of a 10-fold molar excess of TCMDC-135051 (20μM). Staurosporine was used as a positive control or 2% DMSO as a vehicle control. Data was measured in triplicate with repeats indicated in parenthesis. (**B)** Concentration-response curve of inhibition of PRPF4B activity in the presence of TCMDC-135051 (co-purified with trifluoroacetic acid), Compound-A or trifluoroacetic acid (TFA). Data was measured in duplicate. Compound A curve was calculated using the logistic non-linear regression analysis implemented in GraphPad Prism, while fitting for TFA and TCMDC-135051 was generated as a linear regression using the same software. Data shown is the mean ± SEM of three independent experiments.

**Fig. S5. TCMDC-135051 activity against P*f*CDPK1 and *Pf*PKG**

Gel based assay of the phosphorylation of myelin basic protein (MBP) by **(A)** *Pf*CDPK1, **(B)** *Pf*PKG and **(C)** *Pf*CLK3. The top gel is an autoradiograph and the bottom a Commassie stain of the same gel as a loading control. The position of MBP and auto-phosphoryated kinase and the recombinant kinase is shown.

**Fig. S6. Series of related molecules identified from HTS as *Pf*CLK3 inhibitors**

TR-FRET assay of *Pf*CLK3 activity was used to generate concentration inhibition curves of TCMDC-135049, TCMDC-135050 and TCMDC-135051. Shown is the mean of three experiments ± S.E.M).

**Fig. S7. Enzymatic kinetics of *Pf*CLK3 and the G449P variant and growth rates of mutant parasites expressing G449P.**

**(A)** Measure of recombinant *Pf*CLK3 and G449P at various concentrations of ATP. The data shown is the mean ±S.E.M of at least three independent experiments. **(B)** The multiplication rate of the A3 strain of G449P mutant parasites was tested together with that parent 3D7 strain. The starting parasitaemia was 0.3% and the increase in parasitaemia measured after 52 hours (one cycle). Multiplication rate=parasitaemia at 52 hours(%)/initial parasitaemia(%). The data presented is the mean ±S.E.M of three determinations.

**Fig. S8. Biological function of genes that are down regulated by PfCLK3 inhibition.**

Gene ontology enrichment analysis showing biological function of genes significantly down regulated by TCMDC-135051 treatment in Dd2 parasites. Biological functions with FDR <0.05 ((calculated using the Benjamini Hochberg method) are shown (see; Supplementary Table S5 full data set).

**Fig. S9. Comparison of the enzyme kinetics of *Pv*CLK3 and *Pb*CLK3.**

Measure of recombinant *Pf*CLK3 and *Pb*CLK3 at various concentrations of ATP. The data shown is the mean ±S.E.M of at least three independent experiments.

**Fig. S10. Inhibition of PvCLK3 and PbCLK3 by TCMDC-135051.**

TR-FRET in vitro kinase assays were conducted on full length recombine **(a)** PvCLK3 and **(b)** PbCLK3 in the presence of various concentrations of TCDMC-135051. Shown at the mean ± SEM of three independent experiments.

**Fig. S11. Activity of TCMDC-135051 at liver invasion and sporozoite development.**

Concentration effect curve of TCMDC-135051 on *P. berghei* sporozoite development. The data shown are the mean ±S.E.M of at least three independent experiments.

**Fig. S12. Death curves of Pf2004 blood stage and stage II gametocytes in response to TCDMC-135051.**

Parasite viability assays were conducted on **(A)** Pf2004 parasite strain at the asexual blood stage and **(B)** Pf2004 stage II gametocytes. Shown at the mean ± SEM of three independent experiments.

**Fig. S13. Inhibition of *Pf*CLK3 at stage V gametocytes reduces transmission to the mosquito vector.**

Concentration effect of exposure of *P. falciparum* (clone 3D7) stage V gametocytes to TCMDC-135051 on **(A,B)** gametocyte (GC) numbers in culture, **(C,D)** exflagellation, and **(E,F)** prevalence of infection of *An. coluzzii* mosquitoes. The top row of graphs **(A,C,E)** show the mean ±SEM of 4 independent experiments. The lower panels show the predicted effects of drug concentrations according to the maximal GLMM with the shaded area indicating 95% confidence intervals. From the GLMM analysis the approximate $EC_{50}$ values were calculated.

**Supplementary Tables**

**Supplementary Table S1. Compound Screen.**

Hits from the primary single dose HTS (2838) and compounds contained in the MMV-malaria box (259) were used to generate concentration inhibitor curves. Shown are pIC50 values against PfCLK3, PfCLK1, PvCLK3 and hCLK2 (sheet 1). These data are divided into data associated with TCAMs/GSK compounds (sheet 2), PKIS compounds (sheet 3), MRCT compounds (sheet 4) and MMV compounds (sheet 5).

**Supplementary Table S2. Transcription changes in parent *P. falciparum* strain Dd2 following treatment with TCMDC-135051.**

*Sheet 1* – Statistically significant changes (t-test n=4) in transcript levels following treatment of Dd2 parasites at trophozoite stage with TCMDC-135051 (1μM for 60 mins). Shown are the probes used and changes associated with each of the probes. *Sheet 2* – Summary of the probes that reveal significantly down-regulated genes following TCMDC-135051 treatment. *Sheet 3* - Summary of the genes that are significantly down-regulated following TCMDC-135051 treatment. *Sheet 4* - Summary of the probes that reveal significantly up-regulated genes following TCMDC-135051 treatment. *Sheet 5*- Summary of the genes that are significantly up-regulated following TCMDC-135051 treatment.

**Supplementary Table S3. Transcription changes in the resistant parasite strain TM051C following treatment with TCMDC-135051.**

*Sheet 1* – Statistically significant changes (t-test n=4) in transcript levels following treatment of TM051C parasites at trophozoite stage with TCMDC-135051 (1μM for 60 mins). Shown

are the probes used and changes associated with each of the probes. *Sheet 2* – Summary of the probes that reveal significantly down-regulated genes following TCMDC-135051 treatment. *Sheet 3* - Summary of the genes that are significantly down-regulated following TCMDC-135051 treatment. *Sheet 4* - Summary of the probes that reveal significantly up-regulated genes following TCMDC-135051 treatment. *Sheet 5*- Summary of the genes that are significantly up-regulated following TCMDC-135051 treatment.

**Supplementary Table S4. Transcription changes designated as a result of on-target inhibition of *Pf*CLK3 and a comparison with essential *Plasmodium falciparum* genes.**

Subtracting the genes where transcription was significantly changed following treatment with TCMDC-135051 (1μM for 60 mins) in TM051C parasites with those changed in Dd2 parasites revealed the "on target" transcriptional changes associated with inhibition of PfCLK3. *Sheet 1* – On target up-regulated genes. *Sheet–2* Identification (highlighted) of the on target up regulated genes that are essential for parasite blood stage survival. *Sheet 3*- On target down-regulated genes. *Sheet 4*- Identification (high-lighted) of the on target down regulated genes that are essential for parasite blood stage survival.

**Supplementary Table S5. Gene ontology analysis of on-target down regulated genes following inhibition of *Pf*CLK3 in Dd2 parasites.**

Gene ontology enrichment analysis was carried out on genes that were significantly down-regulated by *Pf*CLK3 inhibition. GO terms with $P < 0.05$ (derived from the Fisher's Exact test) and with FDR values <0.05 (calculated using the Benjamini Hochberg method) are shown on *sheet 1*, whilst all Go terms with a $P<0.05$ are shown on *sheet 2*. From left to right, columns show: the GO term id, the GO term name, the number of genes in the background

annotated with this GO term, the number of genes significantly downregulated by *Pf*CLK3 inhibition annotated with this GO term, a list of the downregulated genes annotated with this GO term, the percentage of genes in the background annotated with this GO term that also appear in the list of downregulated genes, the fold enrichment of the GO term in the downregulated gene list, an odds ratio, a p-value and the FDR.